HiLL PUBLISHING

Journal of Applied Mathematics and Computation, 2023, 7(4), 426-442
https://www.hillpublisher.com/journals/JAMC/
ISSN Online: 2576-0653
ISSN Print: 2576-0645

About Radiation of Sliding Waves

Vladimir Arabadzhi

Institute of Applied Physics, Russian Academy of Sciences, Nizhny Novgorod, Russia.

How to cite this paper: Vladimir Arabadzhi. (2023) About Radiation of Sliding Waves. *Journal of Applied Mathematics and Computation*, 7(4), 426-442.
DOI: 10.26855/jamc.2023.12.002

Received: October 31, 2023
Accepted: November 23, 2023
Published: December 19, 2023

***Corresponding author:** Vladimir Arabadzhi, Institute of Applied Physics, Russian Academy of Sciences, Nizhny Novgorod, Russia.

Abstract

It is shown that for waves of different physical nature (sound waves, gravitational surface waves in a liquid, electromagnetic waves) of the two field components, included as factors in the Poynting vector, only one component, given at the boundary, provides a resonant increase in the surface power flux density of the sliding wave radiation to infinity, as the spatial frequency of the boundary excitation approaches to the wavenumber in the medium (and a jump to zero after any exceeding the wavenumber of the medium). Also, it is shown that at the boundary with given travelling in space phase of normal vibrational velocities (or a tangentional electric field) arises the constant in time and along the boundary component of the tangential force of the radiation reaction (the force of wave thrust or the force of wave resistance, as following from concrete statement of the boundary value problem), which is not caused by nonlinearity of the medium and proportional to the radiated power, which can be large near resonance. The similarities and the cases of sliding waves of different physical natures and patterns of different types are discussed. The influence of the finite length of the radiating boundary and its curvature on the magnitude of the resonance is studied. It is shown that in the case of a linear equidistant chain of three-dimensional acoustic monopoles, the resonance is completely absent.

Keywords

Radiating of pattern, spatial frequency, temporal frequency, resonance radiation, boundary condition, phased array antenna mode, towed static structure mode, wave drive, wave resistance, sound waves, gravitational surface waves in liquid, electromagnetic waves

Introduction

The radiation of waves by boundaries was considered in many classical works (see, for example, [1-9]). In [7-9], many variants of fields created by traveling distributions of sources are given, but no resonance effects were found, because it was the given sources that were considered there and not the given fields at the boundary, that is, the “traveling” terms on the right side of the wave equation or boundary conditions. Only [10] contains the statement considered below of the two-dimensional problem for sound waves: at harmonic on $"x"$, $"t"$ excitation $\Phi_0 = \exp(i\omega_0 t - ih_0 x)$ ($|x| < L_0 = \infty$, $|t| < T_0 = \infty$) of a flat boundary $z = 0$ in contact with an inviscid compressible half-space $z \geq 0$, at temporal and spatial frequencies ω_0 and h_0. In the same work [10], a fundamental difference in sound fields was noted when the boundary was excited by a given normal velocity or by a given pressure. However, for some reason the author did not pay attention to the resonant dependence of the radiated wave amplitude on h_0: infinite growth at $k_0 > h_0 \to k_0$ and jump to zero at $h_0 = k_0 + 0$ when scanning along h_0, where $k_0 = \omega_0 / c_{0a}$ is the wave number in the medium, c_{0a} is the speed of

sound in the medium. Below, we study (see [10, 11]) the energy output of the boundary (as also the tangential force of the reaction of the radiated field to the boundary that generated it) in the form of radiation of waves generated by a certain pattern with a spatiotemporal framework Φ_0 and a phasor $\mathbf{h}_0$ ($|\mathbf{h}_0| = h_0$), denoting the direction of the linear growth of the field phase, specified on the border of the pattern. A pattern (see below patterns $\hat{S}_{0V}, \hat{S}_{0P}, \hat{S}_{0Vg}, \hat{S}_{0Pg}, \hat{S}_{0J}, \hat{S}_{0E}, \hat{S}_{0\tilde{V}}$, $\hat{S}_{0\tilde{V}g}, \hat{S}_{0\tilde{E}}, \hat{S}_{1V}, \hat{S}_{2V}, \hat{S}_{3V}, \hat{S}_{4V}, \hat{S}_{5V}$) is a certain design of a radiator (antenna) with a given traveling field distribution supported in some way on its surface.

1. Flat Acoustic Patterns ($\hat{S}_{0V}, \hat{S}_{0P}, L_0 = \infty$)

As an initial pattern (which, following the work [10] by M.A. Isakovich, gave rise to interest in studying the others) we consider a flat ($z = 0$) two-dimensional ($\partial/\partial y = 0$) pattern with the width $L_0 = \infty$ along "x". The sound field in a compressible inviscid linear two-dimensional medium is described by the wave potential $\varphi(x,z,t)$ satisfying the equation $\varphi''_{xx} + \varphi''_{zz} = c_{0a}^{-2}\varphi''_{tt}$. The velocities $\upsilon_x(x,z,t)$, $\upsilon_z(x,z,t)$ (along the axes "x" and "z") of the particles of the medium and the acoustic pressure $p(x,z,t)$ are determined through the acoustic potential $\varphi(x,z,t)$: $\upsilon_x = -(\partial/\partial x)\varphi$, $\upsilon_z = -(\partial/\partial z)\varphi$, $p = \rho_0(\partial/\partial t)\varphi = i\omega_0\rho_0\varphi$. At the boundary $z = 0$ we set either the normal vibrational speed (pattern $\hat{S}_{0V}$) $-[\varphi'_z]_{z=0} = \Phi_0 V_{0V}$, having received the potential $\varphi = \varphi_{0V}$, or we set the sound pressure (pattern $\hat{S}_{0P}$) $i\omega_0\rho_0[\varphi]_{z=0} = \Phi_0 P_{0P}$, having obtained the potential $\varphi = \varphi_{0P}$. The functions φ_{0V} and φ_{0P} have the following form:

$$\varphi_{0V} = \mathbf{I}[k_0 - |h_0|]\frac{-i}{k_0}\frac{\exp(-iz\sqrt{k_0^2 - h_0^2})}{\sqrt{1-(h_0/k_0)^2}}\Phi_0 V_{0V} + \mathbf{I}[|h_0| - k_0]\frac{1}{k_0}\frac{\exp(-z\sqrt{h_0^2 - k_0^2})}{\sqrt{(h_0/k_0)^2 - 1}}\Phi_0 V_{0V},$$

$$\varphi_{0P} = \mathbf{I}[k_0 - |h_0|]\frac{1}{i\omega_0\rho_0}\exp(-iz\sqrt{k_0^2 - h_0^2})\,\Phi_0 P_{0P} + \mathbf{I}[|h_0| - k_0]\frac{1}{i\omega_0\rho_0}\exp(-z\sqrt{h_0^2 - k_0^2})\,\Phi_0 P_{0P},$$

где $\mathbf{I}[\xi > 0] = 1$, $\mathbf{I}[\xi < 0] = 0$. Next, we obtain the complex Poynting vectors of the power flux density at a frequency ω_0 on the surface $z = 0$) corresponding to the potentials φ_{0V}, φ_{0P} of patterns $\hat{S}_{0V}$, $\hat{S}_{0P}$: $\mathbf{W}_{0V} = [(i\omega_0\rho_0\varphi_{0V})^*(-\nabla\varphi_{0V})]/2$ and $\mathbf{W}_{0P} = [(i\omega_0\rho_0\varphi_{0P})^*(-\nabla\varphi_{0P})]/2$, where $\nabla = \mathbf{x}_0(\partial/\partial x) + \mathbf{z}_0(\partial/\partial z)$, and $\mathbf{x}_0, \mathbf{z}_0$ are unit vectors along the axes "x","z".

Now let us formulate the power flows (at $z \geq 0$) of patterns $\hat{S}_{0V}$ and $\hat{S}_{0P}$, normalized to $\mathrm{w}_{0V} = \mathrm{Re}[\mathbf{z}_0\mathbf{W}_{0V}(h_0 = 0)] = |V_{0V}|^2\rho_0 c_{0a}/2$ and $\mathrm{w}_{0P} = \mathrm{Re}[\mathbf{z}_0\mathbf{W}_{0P}(h_0 = 0)] = |P_{0P}|^2/2\rho_0 c_{0a}$ respectively:

$$(\mathbf{z}_0\mathbf{W}_{0V})/\mathrm{w}_{0V} = \overline{G}^{z}_{0V} + i\overline{\overline{G}}^{z}_{0V},\quad (\mathbf{x}_0\mathbf{W}_{0V})/\mathrm{w}_{0V} = \overline{G}^{x}_{0V} + i\overline{\overline{G}}^{x}_{0V},$$

$$(\mathbf{z}_0\mathbf{W}_{0P})/\mathrm{w}_{0P} = \overline{G}^{z}_{0P} + i\overline{\overline{G}}^{z}_{0P},\quad (\mathbf{x}_0\mathbf{W}_{0P})/\mathrm{w}_{0P} = \overline{G}^{x}_{0P} + i\overline{\overline{G}}^{x}_{0P},$$

$$\overline{G}^{x}_{0V} = \mathrm{Re}(\mathbf{x}_0\mathbf{W}_{0V})/\mathrm{w}_{0V},\quad \overline{\overline{G}}^{x}_{0V} = \mathrm{Im}(\mathbf{x}_0\mathbf{W}_{0V})/\mathrm{w}_{0V},\quad \overline{G}^{z}_{0V} = \mathrm{Re}(\mathbf{z}_0\mathbf{W}_{0V})/\mathrm{w}_{0V},\quad \overline{\overline{G}}^{z}_{0V} = \mathrm{Im}(\mathbf{z}_0\mathbf{W}_{0V})/\mathrm{w}_{0V},$$

$$\overline{G}^{x}_{0P} = \mathrm{Re}(\mathbf{x}_0\mathbf{W}_{0P})/\mathrm{w}_{0P},\quad \overline{\overline{G}}^{x}_{0P} = \mathrm{Im}(\mathbf{x}_0\mathbf{W}_{0P})/\mathrm{w}_{0P},\quad \overline{G}^{z}_{0P} = \mathrm{Re}(\mathbf{z}_0\mathbf{W}_{0P})/\mathrm{w}_{0P},\quad \overline{\overline{G}}^{z}_{0P} = \mathrm{Im}(\mathbf{z}_0\mathbf{W}_{0P})/\mathrm{w}_{0P}.$$

The values $\overline{G}^{z}_{0V}$, $\overline{G}^{z}_{0P}$, can be interpreted as the normalized radiation resistance of the patterns $\hat{S}_{0V}$ and $\hat{S}_{0P}$. And the boundary $z = 0$, together with the waveguide half-space $z \geq 0$, can be interpreted as a low pass filter in the space of spatial frequencies with a "transparency band" $|h_0| < k_0$, see Fig. 1a. Next, we obtain the normalized energy characteristics of the pattern $\hat{S}_{0V}$ (as well as and $\hat{S}_{0Vg}, \hat{S}_{0E}$, see Sections 2 and 3) averaged over the period $2\pi/\omega_0$:

$$\overline{G}^{z}_{0V} = \left[1-(h_0/k_0)^2\right]^{-1/2}\mathbf{I}\left[k_0-\left|h_0\right|\right],\quad \overline{\overline{G}}^{z}_{0V} = \left[(h_0/k_0)^2-1\right]^{-1/2}\exp\left[-2z\sqrt{h_0^2-k_0^2}\right]\ \mathbf{I}\left[\left|h_0\right|-k_0\right],\quad \overline{\overline{G}}^{x}_{0V} = 0, \tag{3}$$

$$\overline{G}^{x}_{0V} = (h_0/k_0)\left[1-(h_0/k_0)^2\right]^{-1}\mathbf{I}\left[k_0-\left|h_0\right|\right] + (k_0/h_0)\left[1-(k_0/h_0)^2\right]^{-1}\exp\left[-2z\sqrt{h_0^2-k_0^2}\right]\ \mathbf{I}\left[\left|h_0\right|-k_0\right]. \tag{4}$$

Analogously for the pattern $\hat{S}_{0P}$ (as well as $\hat{S}_{0Pg}$, $\hat{S}_{0J}$, see sections 2, 3):

$$\overline{G}^{z}_{0P} = \sqrt{1-(h_0/k_0)^2}\ \mathbf{I}\left[k_0-\left|h_0\right|\right],\quad \overline{G}^{x}_{0P} = (h_0/k_0)\ \mathbf{I}\left[k_0-\left|h_0\right|\right] + (h_0/k_0)\ \exp\left[-2z\sqrt{h_0^2-k_0^2}\right]\ \mathbf{I}\left[\left|h_0\right|-k_0\right], \tag{5}$$

$$\overline{\overline{G}}^{z}_{0P} = \sqrt{(h_0/k_0)^2-1}\ \exp\left[-2z\sqrt{h_0^2-k_0^2}\right]\ \mathbf{I}\left[\left|h_0\right|-k_0\right],\quad \overline{\overline{G}}^{x}_{0P} = 0. \tag{6}$$

For patterns with $L_0=\infty$ ($\hat{S}_{0V}, \hat{S}_{0P}, \hat{S}_{0Vg}, \hat{S}_{0Pg}, \hat{S}_{0J}, \hat{S}_{0E}$) the fields of the Poynting vector are either purely imaginary (for $h_0 > k_0$ and $\forall x, z$) or purely real (for $h_0 < k_0$ and $\forall x, z$), but for $L_0 < \infty$ ($\hat{S}_{1V}, \hat{S}_{2V}, \hat{S}_{3V}, \hat{S}_{4V}$), the imaginary and real parts of the Poynting vectors are nonzero for any h_0 (see section 6.1 and Fig. 4a,b). Figures 1a and 1b show the characteristics $\overline{G}^{z}_{0V}, \overline{\overline{G}}^{z}_{0V}$ and $\overline{G}^{z}_{0P}, \overline{\overline{G}}^{z}_{0P}$ of patterns when scanning either by spatial frequency h_0 (when the temporal frequency ω_0 is fixed, Fig. 1a) or by the temporal frequency ω_0 (when the spatial frequency h_0 is fixed, Fig. 1b).

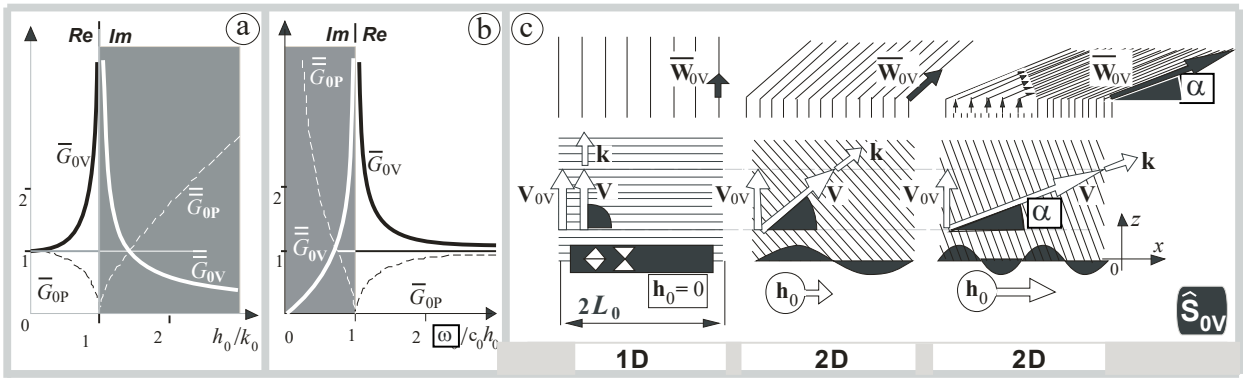

Figure 1. Infinite flat acoustic patterns $\hat{S}_{0V}$, $\hat{S}_{0P}$. Resonances: scanning of active (area Re) and reactive (shaded area Im) characteristics of energy output $\overline{G}^{z}_{0V}, \overline{\overline{G}}^{z}_{0V}$, pattern $\hat{S}_{0V}$, as well as scanning of active and reactive energy output $\overline{G}^{z}_{0P}$, $\overline{\overline{G}}^{z}_{0P}$, (dashed lines) of pattern $\hat{S}_{0P}$ in spatial (a) frequency h_0 (at fixed temporal frequency ω_0) and scanning by temporal (b) frequency ω_0 (at fixed spatial frequency h_0); (c) the geometry of the acoustic pattern and the field of the Poynting vector when scanning the frequency from $h_0 = 0$ to $h_0 = k_0$ and maintaining the particle velocity $\mathbf{V}$ amplitude component V_{0V} normal to the boundary $z = 0$ in the radiated wave.

We see that, the pattern $\hat{S}_{0V}$ has a resonance at $h_0 = \omega_0 / c_{0a} = k_0$, but the pattern $\hat{S}_{0P}$ has no resonance. So, for example, at $h_0 \to k_0$, the surface power flux density of the pattern $\hat{S}_{0V}$ at each point of the boundary $z = 0$ tends to infinity at an arbitrarily small amplitude V_{0V} of its normal velocity. This fact indicates that the growth of the radiated power is promoted by the interaction of all elements of an infinite (both along "x" and along "y") radiating surface $z = 0$ through the sound field in the two-dimensional boundary value problem of the pattern $\hat{S}_{0V}$. Note also that for $\hat{S}_{0V}$ (i.e. at $|x| < L_0 = \infty$), both at $h_0 < k_0$ and at $h_0 > k_0$, there is a nonzero time-constant real power flux $\overline{G}^{x}_{0V}$ in the direction of the phasor $\mathbf{h}_0$ along the axis "x" along the boundary $z = 0$, which is in $(h_0/k_0)\left[1-(h_0/k_0)^2\right]^{-1/2} >> 1$ times

greater than the flux $\overline{G}^{z}_{0\mathrm{V}}(h_0 < k_0)$, although this flux is not directly related (as $\overline{G}^{z}_{0\mathrm{V}}$) to the energy output of boundary. Fig. 1c illustrates an of explosive growth $\overline{G}^{z}_{0\mathrm{V}}$ at $h_0 \to k_0$. Due to the concrete combination of eigenvalues of the boundary value problem in the half-space $z \geq 0$ at $h_0 < k_0$, only a traveling plane wave with an angle α between the wave vector $\mathbf{k}$ ($|\mathbf{k}| = k_0$) and the axis "x" is possible. Therefore, the half-space $z \geq 0$, controlled by the wave equation, is "forced" to increase the particle velocity amplitude $\mathbf{V} \parallel \mathbf{k}$ in $1/\sin\alpha = 1/\sqrt{1-(h_0/k_0)^2} = \overline{G}^{z}_{0\mathrm{V}}$ times (relative to the one-dimensional case $h_0 = 0$, $\alpha = \pi/2$) at $h_0 \to k_0$, in order to ensure the constancy of the particle velocity projection $\mathbf{z}_0\mathbf{V} = V_{0\mathrm{V}}$. Simultaneously with the velocity amplitude, the plane wave pressure amplitude $|P| = |\mathbf{V}|\rho_0 c_0$ increases by the same factor $\overline{G}^{z}_{0\mathrm{V}}$, and the wave intensity increases by a factor of $(\overline{G}^{z}_{0\mathrm{V}})^2$. For any $h_0 > k_0$ (beginning from $h_0 = k_0 + 0$ (region **Im** in Fig. 1a) the intensity of the radiated wave is zero, i.e. $\overline{G}^{z}_{0\mathrm{V}}(h_0 > k_0) = 0$. This kind of dependence is called resonant, but for a pattern $\hat{\mathrm{S}}_{0\mathrm{P}}$ with a given pressure (in contrast to $\hat{\mathrm{S}}_{0\mathrm{V}}$), the resonance described above is absent (see Fig. 1a,b). Therefore, we will no longer consider the pattern $\hat{\mathrm{S}}_{0\mathrm{P}}$ and its analogues in detail. The reverse side of the infinite growth of the surface power density emitted by the pattern $\hat{\mathrm{S}}_{0\mathrm{V}}$ at $h_0 \to k_0$ is the infinite growth of the counteraction, i.e. surface normal force $\Delta\mathbf{F} \parallel \mathbf{z}_0$ density $|\Delta\mathbf{F}|/\Delta S$ with which the half-space $z \geq 0$ resists (in the absence of viscosity) to forced normal vibrations of any little piece ΔS of radiating surface. To illustrate, consider three examples: (a) for a small pulsating hemisphere of radius R_0 ($(k_0 R_0) << 1$) on a rigid flat infinite screen $z = 0$, we obtain $\{|\Delta\mathbf{F}|/\Delta S\}_1 \approx (\rho_0 c_{0a})\ (k_0 R_0)\ (32/3)$; (b) for the pattern $\hat{\mathrm{S}}_{0\mathrm{V}}$ at $h_0 = 0$ we get $\{|\Delta\mathbf{F}|/\Delta S\}_2 = (\rho_0 c_{0a}) >> \{|\Delta\mathbf{F}|/\Delta S\}_1$; (c) and for the same pattern $\hat{\mathrm{S}}_{0\mathrm{V}}$ at $h_0 \to k_0$, we get $\{|\Delta\mathbf{F}|/\Delta S\}_3 = (\rho_0 c_{0a})[1-(h_0/k_0)^2]^{-1/2} >> \{|\Delta\mathbf{F}|/\Delta S\}_2$. Therefore, for example, there is always a spatial frequency $\overline{h}_0$ of excitation of the boundary sufficiently close to k_0 ($|\overline{h}_0 - k_0|/k_0 << 1$), at which the resistance, for example, of an *air half-space* to boundary oscillations will be higher than the resistance of, for example, a *steel half-space* $z \geq 0$ at $h_0 = 0$. On the other hand, the absence of resonance in the pattern $\hat{\mathrm{S}}_{0\mathrm{P}}$ is explained by the fact that any finite pressure at the spatial frequency $h_0 = k_0$ applied to the boundary $z = 0$ is unable to "rock" it, and the compressible medium becomes *dynamically incompressible*. Note that even at $|V_{0\mathrm{V}}|/c_{0a} << 1$, the tangential particle velocity $|\upsilon_x|_{z=0}/c_{0a} = (|V_{0\mathrm{V}}|/c_{0a})\ (h_0/k_0)/\sqrt{1-(h_0/k_0)^2}$ at the boundary $z = 0$ can go beyond the linear model of the medium, *i.e.* $|\upsilon_x|_{z=0}/c_{0a} = (|V_{0\mathrm{V}}|/c_{0a})\ (h_0/k_0)/\sqrt{1-(h_0/k_0)^2} > 1$.

2. Flat patterns for waves on water surface ($\hat{\mathrm{S}}_{0\mathrm{V}}, \hat{\mathrm{S}}_{0\mathrm{P}}, L_0 = \infty$)

The wave potential $\varphi(\mathbf{r}, \omega_0)$ of gravitational surface waves at a frequency in an inviscid incompressible infinitely deep fluid [5] (Fig. 3a) satisfies: (a) the Laplace equation $\varphi''_{\mathrm{xx}} + \varphi''_{\mathrm{yy}} + \varphi''_{\mathrm{zz}} = 0$; (b) the condition $\left[\varphi''_{\mathrm{tt}} - g_0\varphi'_{\mathrm{y}}\right]_{y=0} = 0$ of zero pressure on the free surface $y = 0$ of the liquid; (c) normal velocity $-[\varphi'_{\mathrm{z}}]_{z=0} = \Phi_0 V_{0\mathrm{Vg}} \exp(-k_0 y)$ (pattern $\hat{\mathrm{S}}_{0\mathrm{Vg}}$) on the half-plane ($-\infty \leq x < \infty$, $y \geq 0$, $z = 0$) or pressure $i\omega_0\rho_0[\varphi]_{z=0} = \Phi_0 P_{0\mathrm{Pg}} \exp(-k_0 y)$ (pattern $\hat{\mathrm{S}}_{0\mathrm{Pg}}$), where $k_0 = \omega_0^2/g_0$, g_0 is gravitational acceleration. In the absence of incident waves and when the amplitude of the waves tends to zero with depth $y \to \infty$ it is easy to obtain the wave potentials $\varphi_{0\mathrm{Vg}}(x, y, z, \omega_0)$ and $\varphi_{0\mathrm{Pg}}(x, y, z, \omega_0)$ fields of the patterns $\hat{\mathrm{S}}_{0\mathrm{Vg}}$ and $\hat{\mathrm{S}}_{0\mathrm{Pg}}$. Determining the vectors $\mathbf{W}_{0\mathrm{Vg}}$, $\mathbf{W}_{0\mathrm{Pg}}$ power flux density of patterns $\hat{\mathrm{S}}_{0\mathrm{Vg}}$ and $\hat{\mathrm{S}}_{0\mathrm{Pg}}$ similarly to patterns $\hat{\mathrm{S}}_{0\mathrm{V}}$ and $\hat{\mathrm{S}}_{0\mathrm{P}}$, we obtain expressions

$$\overline{G}^{z}_{0\,Vg}=\overline{G}^{z}_{0\,V},\ \overline{\overline{G}}^{z}_{0\,Vg}=\overline{\overline{G}}^{z}_{0\,V},\ \overline{G}^{x}_{0\,Vg}=\overline{G}^{x}_{0\,V},\ \overline{\overline{G}}^{x}_{0\,Vg}=\overline{\overline{G}}^{x}_{0\,V},\ \overline{G}^{z}_{0\,Pg}=\overline{G}^{z}_{0\,P},\ \overline{\overline{G}}^{z}_{0\,Pg}=\overline{\overline{G}}^{z}_{0\,P},\ \overline{G}^{x}_{0\,Pg}=\overline{G}^{x}_{0\,P},\ \overline{\overline{G}}^{x}_{0\,Pg}=\overline{\overline{G}}^{x}_{0\,P}$$

for the real and imaginary components of the normalized power flux density along the axes "x" and "z", which are basically identical to the corresponding characteristics of patterns $\hat{S}_{0V}$ (with resonance at frequency $h_0=k_0$), $\hat{S}_{0P}$ (no resonance). The only differences are that: (a) the normalization (at $h_0=0$) power values $w_{0\,Vg}=(\rho_0 g_0/2\omega_0)\ \exp[-2k_0 y]\ \left|V_{0\,Vg}\right|^2$ (for the pattern $\hat{S}_{0\,Vg}$) and $w_{0\,Pg}=(\omega_0/2\rho_0 g_0)\ \exp[-2k_0 y]\ \left|P_{0\,Pg}\right|^2$ (for the pattern $\hat{S}_{0\,Pg}$) are functions of depth y; (b) power flows along the axis "y" are characterized by the expressions:

$$\overline{G}^{y}_{0\,Vg}=0,\ \overline{G}^{y}_{0\,Pg}=0,\ \overline{\overline{G}}^{y}_{0\,Vg}(h_0<k_0)=\left[1-(h_0/k_0)^2\right]^{-1},$$

$$\overline{\overline{G}}^{y}_{0\,Vg}(h_0>k_0)=\left[(h_0/k_0)^2-1\right]^{-1}\exp\left[-2z\sqrt{h_0^2-k_0^2}\right],$$

$$\overline{\overline{G}}^{y}_{0\,Pg}(h_0<k_0)=1,\ \overline{\overline{G}}^{y}_{0\,Pg}(h_0>k_0)=\exp\left[-2z\sqrt{h_0^2-k_0^2}\right].$$

Note that, due to the ratio $z_w>>z_a$ of the acoustic impedances of water z_w and air z_a, a traveling water surface gravity wave (at the time frequency ω_0 and with a phasor h_0) of normal velocity at the interface between air and water can provide a boundary condition $-[\varphi'_z]_{z=0}=V_{0V}\exp(i\omega_0 t-ih_0 x)$ for the sound field potential of the pattern $\hat{S}_{0V}$. Thus, at $h_0\to\omega_0/c_a$ (where c_a is the speed of sound in air), an ultra-long surface water wave of very small amplitude V_{0V} can generate powerful ultra-low-frequency infrasound.

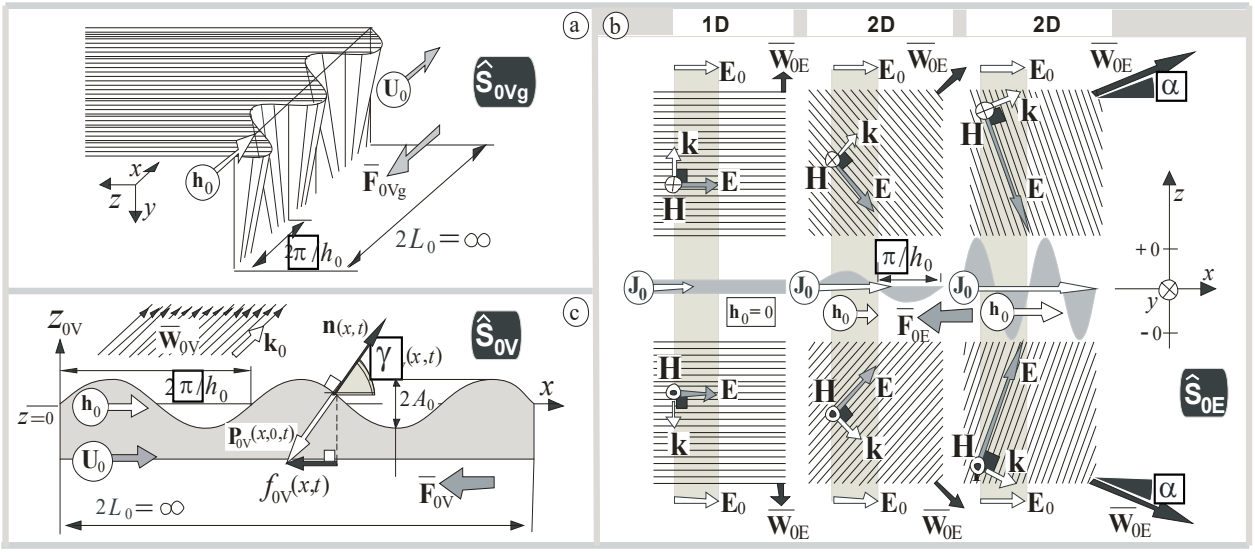

Figure 2. (a) Geometry of patterns $\hat{S}_{0\,Vg}$, $\hat{S}_{0Pg}$, for water waves. (b) Explosive growth of the amplitude E of the electric field of the emitted plane wave at $h_0\to k_0$ in the pattern $\hat{S}_{0E}$ maintaining the constancy of the amplitude E_0 of the tangential electric field at the boundary $z=0$ due to the increase in the current amplitude J_0. (c) Illustration of the origin of the tangential reaction force $f_{0V}(x,t)$ of the pattern $\hat{S}_{0V}$ field on the boundary as a projection of the pressure force $\mathbf{P}_{0V}(x,0,t)$ of the medium on the deviated normal $\mathbf{n}(x,t)$ to the curved boundary with the profile $Z_{0V}(x,t)$. $\overline{\mathbf{F}}_{0Vg}$, $\overline{\mathbf{F}}_{0V}$, $\overline{\mathbf{F}}_{0E}$ —are the wave thrust forces (or wave resistance forces) of the patterns $\hat{S}_{0Vg}$, $\hat{S}_{0V}$, $\hat{S}_{0E}$ (or $\hat{S}_{0\tilde{V}g}$, $\hat{S}_{0\tilde{V}}$, $\hat{S}_{0\tilde{E}}$ with towing velocity $\mathbf{U}_0=\mathbf{x}_0U_0$, see Section 4.2).

3. Flat electromagnetic patterns ($\hat{S}_{0J}$, $\hat{S}_{0E}$, $L_0 = \infty$)

Let us consider the electromagnetic field of the pattern $\hat{S}_{0J}$ [12], excited by an electric current parallel to the axis "x" and uniform along the axis "y" with a surface density $J_{0J}\Phi_0\delta(z)$, where J_{0J} is the complex amplitude, $\delta(z)$ is the delta function. At $h_0 \neq 0$, the current is non-uniform along the axis and generates a surface density of electric charges distribution with a complex amplitude $\sigma_{0J} = (h_0/\omega_0)J_{0J}$ on the plane $z = 0$. The field of the pattern $\hat{S}_{0J}$ is determined by Maxwell's equations and the following additional conditions: (a) the antisymmetry of the fields $E_z(x,-z,t) = -E_z(x,+z,t)$ and $H_y(x,-z,t) = -H_y(x,+z,t)$ relative to $z = 0$ with discontinuities a $[(H_y)_{z=-0} - (H_y)_{z=+0}] = J_{0J}\ \Phi_0$ and $[(E_x)_{z=+0} - (E_x)_{z=-0}]\ \varepsilon_0 = (h_0/\omega_0)\ J_{0J}\ \Phi_0$, where ε_0 is the permittivity of the medium; (b) field symmetry $E_x(x,-z,t) = E_x(x,+z,t)$ with respect to $z = 0$; (c) the finiteness of the fields at $z \to \infty$; (d) absence of incident waves; (e) $\partial/\partial t = i\omega_0$, $\partial/\partial x = ih_0$ for all fields. Thus, there are only three non-zero components $E_x = \mathbf{x}_0\mathbf{E}$, $E_z = \mathbf{z}_0\mathbf{E}$, $H_y = \mathbf{y}_0\mathbf{H}$:

$$E_x(h_0 < k_0) = -\frac{J_{0J}\Phi_0}{2\omega_0\varepsilon_0}\sqrt{k_0^2 - h_0^2}\,\exp\left(-i\,|\,z\,|\,\sqrt{k_0^2 - h_0^2}\right),\quad E_x(h_0 > k_0) = i\,\frac{J_{0J}\Phi_0}{2\omega_0\varepsilon_0}\sqrt{h_0^2 - k_0^2}\,\exp\left(-\,|\,z\,|\,\sqrt{h_0^2 - k_0^2}\right), \quad (7)$$

$$E_z(h_0 < k_0) = -\,\mathrm{sgn}(z)\ \frac{J_{0J}\Phi_0}{2\omega_0\varepsilon_0}\,h_0\,\exp\left(-i\,|\,z\,|\,\sqrt{k_0^2 - h_0^2}\right),\quad E_z(h_0 > k_0) = -\,\mathrm{sgn}(z)\ \frac{J_{0J}\Phi_0}{2\omega_0\varepsilon_0}\,h_0\,\exp\left(-\,|\,z\,|\,\sqrt{h_0^2 - k_0^2}\right), \quad (8)$$

$$H_y(h_0 < k_0) = -\,\mathrm{sgn}(z)J_{0J}\Phi_0\,\exp\left(-i\,|\,z\,|\,\sqrt{k_0^2 - h_0^2}\right)/2,\quad H_y(h_0 > k_0) = -\,\mathrm{sgn}(z)J_{0J}\Phi_0\,\exp\left(-\,|\,z\,|\,\sqrt{h_0^2 - k_0^2}\right)/2, \quad (9)$$

where $\mathrm{sgn}(z > 0) = +1$, $\mathrm{sgn}(z < 0) = -1$. $|\,z > 0\,| = z$, $|\,z < 0\,| = z$. From the Poynting vector $\mathbf{W}_{0J} = [\mathbf{E}, \mathbf{H}^*]/2 = (\mathbf{z}_0/2)E_xH_y^* - (\mathbf{x}_0/2)E_zH_y^*$ of the pattern $\hat{S}_{0J}$, we obtain energy characteristics $\overline{G}_{0J}^x = \mathrm{Re}(\mathbf{x}_0\mathbf{W}_{0J})/w_{0J}$, $\overline{\overline{G}}_{0J}^x = \mathrm{Im}(\mathbf{x}_0\mathbf{W}_{0J})/w_{0J}$, $\overline{G}_{0J}^z = \mathrm{Re}(\mathbf{z}_0\mathbf{W}_{0J})/w_{0J}$, $\overline{\overline{G}}_{0J}^z = \mathrm{Im}(\mathbf{z}_0\mathbf{W}_{0J})/w_{0J}$, (where $w_{0J} = \mathrm{Re}\{\mathbf{z}_0\mathbf{W}_{0J}(h_0 = 0)\} = |J_{0J}|^2/8\omega_0\varepsilon_0$) identical (at $z > 0$ and $\forall h_0$) to the corresponding characteristics of the pattern $\hat{S}_{0P}$ (without resonance at $h_0 = k_0$): $\overline{G}_{0J}^x = \overline{G}_{0P}^x$, $\overline{\overline{G}}_{0J}^x = \overline{\overline{G}}_{0P}^x$, $\overline{G}_{0J}^z = \overline{G}_{0P}^z$, $\overline{\overline{G}}_{0J}^z = \overline{\overline{G}}_{0P}^z$ (the same characteristics are also obtained for a flat pattern) turn with a given magnetic field H_y). From the expressions of the fields E_x, E_z, H_y via the current J_{0J}, we obtain the complex amplitude

$$J_{0E} = J_{0E}(E_{0E}) = -2\omega_0\varepsilon_0E_{0E}\left[(k_0^2 - h_0^2)^{-1/2}\mathbf{I}(k_0^2 - h_0^2) + i\ (h_0^2 - k_0^2)^{-1/2}\mathbf{I}(h_0^2 - k_0^2)\right] \quad (10)$$

of the excitation current of the pattern $\hat{S}_{0E}$, which provides a given distribution $(E_x)_{z=0} = (E_x)_{z=\pm0} = ((\mathbf{h}_0/h_0)\mathbf{E})_{z=0} = \Phi_0E_{0E}$ of the tangential electric field for any h_0. Note that the given (field-independent and not related to conductivity) current is transparent and allows incident waves (which are absent in (7)-(9)) to change the field at the boundary $z = 0$, but setting exactly the field (despite incident waves, for example) on boundary $z = 0$ makes this border completely reflective of the incident waves and opaque. Based on the Poynting vector $\mathbf{W}_{0E} = [\mathbf{E}(J_{0J}(E_{0E})), \mathbf{H}^*(J_{0J}(E_{0E}))]/2$, we obtain for the pattern the energy characteristics $\overline{G}_{0E}^x = \mathrm{Re}(\mathbf{x}_0\mathbf{W}_{0E})/w_{0E}$, $\overline{\overline{G}}_{0E}^x = \mathrm{Im}(\mathbf{x}_0\mathbf{W}_{0E})/w_{0E}$, $\overline{G}_{0E}^z = \mathrm{Re}(\mathbf{z}_0\mathbf{W}_{0E})/w_{0E}$, $\overline{\overline{G}}_{0E}^z = \mathrm{Im}(\mathbf{z}_0\mathbf{W}_{0E})/w_{0E}$ (where $w_{0E} = |E_{0E}|^2\sqrt{\varepsilon_0/\mu_0}/2$, μ_0 is the magnetic permeability of the medium), identical (for $z > 0$ and any h_0) to characteristics of the acoustic pattern $\hat{S}_{0V}$ with resonance at $h_0 = k_0$: $\overline{G}_{0E}^x = \overline{G}_{0V}^x$, $\overline{\overline{G}}_{0E}^x = \overline{\overline{G}}_{0V}^x$, $\overline{G}_{0E}^z = \overline{G}_{0V}^z$, $\overline{\overline{G}}_{0E}^z = \overline{\overline{G}}_{0V}^z$. The explosive growth of the radiation (of $\hat{S}_{0E}$) at $h_0 \to k_0$ is shown in Fig. 3 as a necessity (similar to $\hat{S}_{0V}$, Fig. 1c) to support a projection E_{0E} of the

electric field on "x" (moreover, $(E_{0\mathrm{E}}\mathbf{x}_0) \uparrow\uparrow \mathbf{h}_0$), increasing the current amplitude $J_{0\mathrm{E}}(E_{0\mathrm{E}})$.

4. Radiation reaction

The transfer of mechanical momentum by the power flux of radiated waves is called the problem of wave momentum [13], the study of which continues from the experience of Lebedev [14] to the present day. The point is that in many boundary value problems with the radiation of waves of different physical nature, a time-constant reaction force arises (similar to the jet thrust of a rocket with respect to the gas flowing out of the nozzle), equal to the wave energy flux divided by the phase velocity of the wave. This force manifests itself as an experimental or analytical phenomenon in specific boundary value problems: a volumetric mechanical impulse transferred during the propagation of a plane sound wave in a compressible inviscid gas, taking into account the second order of its dynamics [15, 16]; the force of light pressure on the mirror during reflection [14]. We will consider a constant in "x" and "t" a force tangential to the radiating boundary $z = 0$ and proportional to the resonantly increasing power of the radiated grazing wave at $h_0 \to k_0$.

4.1 Wave drive of a phased array antenna

In this section (as well as in sections 1-3), we will consider patterns $\hat{\mathrm{S}}_{0\mathrm{V}}, \hat{\mathrm{S}}_{0\mathrm{Vg}}, \hat{\mathrm{S}}_{0\mathrm{E}}$ as phased antenna arrays (PAA) with a given distribution of amplitudes and phases of field excitation by array elements resting in the tangential direction.

4.1.1. Sound waves pattern $\hat{\mathrm{S}}_{0\mathrm{V}}$

For $(V_0 \neq 0) \cap (h_0 \neq 0)$, the pattern $\hat{\mathrm{S}}_{0\mathrm{V}}$ boundary $z = 0$ (see Section 1) is transformed into a sinusoidal profile with a complex amplitude $\tilde{\gamma}_{0\mathrm{V}} = (h_0 / \omega_0)\ V_0 << 1$ of the angle (see Fig. 2b) between the normal $\mathbf{n}(x,t)$ ($|\mathbf{n}| = 1$) to the profile (at the point x and t at the moment) and the vector $\mathbf{x}_0$. An inviscid medium applied to the profile of the boundary produces the pressure $\mathbf{P}(x,t) = -p_{0\mathrm{V}}(x,0,t)\mathbf{n}(x,t)$ of a sound field $p_{0\mathrm{V}}(x,z,t)$ with a nonzero projection $f_{0\mathrm{V}}(x,t) = -p_{0\mathrm{V}}(x,0,t)\ \gamma_{0\mathrm{V}}(x,t) \neq 0$ onto the axis "x". If $h_0 < k_0$ the product $(\tilde{p}_{0\mathrm{V}}) * \tilde{\gamma}_{0\mathrm{V}}/\mathbf{2}$ of complex amplitudes of pressure $p_{0\mathrm{V}}(x,t) = \tilde{p}_{0\mathrm{V}}\Phi_0(x,t)$ and slope $\gamma_{0\mathrm{V}}(x,t) = \tilde{\gamma}_{0\mathrm{V}}\Phi_0(x,t)$ has a real part $\overline{F}_{0\mathrm{V}} \neq 0$, then it corresponds to the amplitude $\overline{F}_{0\mathrm{V}}$ of power oscillations (at frequency $2\omega_0$) relative to the average (at period $2\pi/\omega_0$ or $2\pi/h_0$) value $< f_{0\mathrm{V}} >= \overline{F}_{0\mathrm{V}} = \mathrm{Re}[(\tilde{p}_{0\mathrm{V}}) * \tilde{\gamma}_{0\mathrm{V}}]/2 = \mathrm{Re}(\mathbf{z}_0\mathbf{W}_{0\mathrm{V}})/(\omega_0/h_0)$. At $h_0 > k_0$, we have $\overline{F}_{0\mathrm{V}} = 0$, and a non-zero value $\overline{\overline{F}}_{0\mathrm{V}} \neq 0$ corresponds to the oscillation amplitude (at frequency $2\omega_0$) $\overline{\overline{F}}_{0\mathrm{V}} = \mathrm{Im}[(\tilde{p}_{0\mathrm{V}}) * \tilde{\gamma}_{0\mathrm{V}}]/2 = \mathrm{Im}(\mathbf{z}_0\mathbf{W}_{0\mathrm{V}})/(\omega_0/h_0)$ of the tangential force relative to zero. Figure 3d shows the dimensionless surface densities of tangential forces $\bar{\mathrm{f}}_{0\mathrm{V}} = \overline{F}_{0\mathrm{V}}/(\mathrm{w}_{0\mathrm{V}}/c_{0a}) = (h_0/k_0)\overline{G}^{z}_{0\mathrm{V}}(h_0/k_0)$, $\bar{\bar{\mathrm{f}}}_{0\mathrm{V}} = \overline{\overline{F}}_{0\mathrm{V}}/(\mathrm{w}_{0\mathrm{V}}/c_{0a}) = (h_0/k_0)\overline{\overline{G}}^{z}_{0\mathrm{V}}(h_0/k_0)$
(where $\mathrm{w}_{0\mathrm{V}} = |V_{0\mathrm{V}}|^2 \rho_0 c_{0a}/2$) of the reaction force amplitudes as functions of h_0/k_0.

4.1.2. Waves on the water surface (pattern $\hat{\mathrm{S}}_{0\mathrm{Vg}}$)

The same reasoning as in Section 4.1.1 can be done for a pattern $\hat{\mathrm{S}}_{0\mathrm{Vg}}$ with a vertical boundary $z = 0$ (in an infinitely deep inviscid fluid (Fig. 3a), on which the distribution $\Phi_0 V_0 \exp(-k_0 y)$ of normal vibrational velocities is specified with the variables replaced by their analogs: $p_{0\mathrm{V}}(x,t) \Rightarrow p_{0\mathrm{Vg}}(x,y,t) = \tilde{p}_{0\mathrm{Vg}}\Phi_0(x,t)\exp(-k_0 y)$, $\gamma_{0\mathrm{V}}(x,t) \Rightarrow \gamma_{0\mathrm{Vg}}(x,y,t) = \tilde{\gamma}_{0\mathrm{Vg}}\Phi_0(x,t)\exp(-k_0 y)$ and obtain similar expressions for the exponentially decreasing in depth surface density of the tangential force:

$$\overline{F}_{0\mathrm{Vg}} = \mathrm{Re}[(\tilde{p}_{0\mathrm{Vg}}) * \tilde{\gamma}_{0\mathrm{Vg}}]/2 = \frac{\mathrm{Re}(\mathbf{z}_0\mathbf{W}_{0\mathrm{Vg}})}{(\omega_0/h_0)} =< f_{0\mathrm{Vg}} >,\quad \overline{\overline{F}}_{0\mathrm{Vg}} = \mathrm{Im}[(\tilde{p}_{0\mathrm{Vg}}) * \tilde{\gamma}_{0\mathrm{Vg}}]/2 = \frac{\mathrm{Im}(\mathbf{z}_0\mathbf{W}_{0\mathrm{Vg}})}{(\omega_0/h_0)}.$$

Fig. 3d presents the dimensionless quantities $\bar{f}_{0Vg} = \overline{F}_{0Vg}/(w_{0Vg}/c_{0g}) == (h_0/k_0)\overline{G}^z_{0V}(h_0/k_0)$, $\bar{\bar{f}}_{0Vg} = \bar{\bar{F}}_{0Vg}/(w_{0Vg}/c_{0g}) == (h_0/k_0)\overline{\overline{G}}^z_{0V}(h_0/k_0)_{0V}$ as functions of h_0/k_0, where $w_{0Vg} = (\rho_0 g_0/2\omega_0)\ \exp[-2k_0 y]\ \left|V_{0Vg}\right|^2$.

4.1.3. Electromagnetic waves (pattern $\hat{S}_{0E}$)

Next, consider the electromagnetic pattern $\hat{S}_{0E}$. The current $J_{0E}(E_{0E})$ provides a constant (for any h_0) amplitude of the tangential "x" component of the electric field E_{0E} on the surface $z = 0$. The magnetic field $\mathbf{H}$ of the pattern $\hat{S}_{0E}$ acts on the current J_{0E} by the Ampere force $\mathbf{F}_A \sim [\mathbf{x}_0 J_{0E}, \mathbf{H}]_{z=0}$, but the total Ampere force (from the sides $z = +0$ and $z = -0$) is equal to zero.

The electric field $\mathbf{E}$ generated by the same current J_{0E} acts on the distribution $\sigma_{0E}(x,t) = (h_0/\omega_0)J_{0E}(x,t)$ of electric charges by a non-zero Coulomb force $\mathbf{F}_Q = \sigma_{0E}\mathbf{E} = f_{0E}(x,t) = \sigma_{0E}(x,t)\{\mathbf{E}(J_{0E}(x,t))\}_{\mathbf{z}=0}$, in which the charge distribution $\sigma_{0E} = (h_0/\omega_0)J_{0E}$ is analogous to the angle $\gamma_{0V}(x,t)$ of inclination of the boundary in pattern $\hat{S}_{0V}$, and the given electric field $E_{0E}(x,0,t)$ is analogous to the acoustic pressure $p_{0V}(x,t)$ in the pattern $\hat{S}_{0V}$ (section 4.4.1). Similarly to the pattern $\hat{S}_{0V}$, we write the amplitude $\overline{F}_{0E}$ of oscillations of the surface density of the tangential force near its average value $< f_{0E} >= \overline{F}_{0E} \neq 0$ at $h_0 < k_0$ and the amplitude $\overline{\overline{F}}_{0E}$ of oscillations (near zero at $h_0 > k_0$ and $\overline{F}_{0E} = 0$): $\overline{F}_{0E} = (1/2)\,\mathrm{Re}[(\sigma_{0E}) * E_0] = \mathrm{Re}(\mathbf{z}_0\mathbf{W}_{0E})/(\omega_0/h_0)$, $\overline{\overline{F}}_{0E} = (1/2)\,\mathrm{Im}[(\sigma_{0E}) * E_{0E}] = \mathrm{Im}(\mathbf{z}_0\mathbf{W}_{0E})/(\omega_0/h_0)$. Fig. 3d presents the dimensionless quantities $\bar{f}_{0E} = \overline{F}_{0E}/(w_{0E}/c_{0e}) == (h_0/k_0)\overline{G}^z_{0V}(h_0/k_0)$, $\bar{\bar{f}}_{0E} = \overline{\overline{F}}_{0E}/(w_{0E}/c_{0e}) == (h_0/k_0)\overline{\overline{G}}^z_{0V}(h_0/k_0)$, as functions of h_0/k_0, where $w_{0E} = \left|E_{0E}\right|^2\sqrt{\varepsilon_0/\mu_0}$ is the sum of the radiation power densities on both sides of the boundary $z = 0$.

4.2 Wave resistance

Now, instead of setting a running (along "x" and "t") excitation Φ_0 of fixed (along "x") patterns $\hat{S}_{0V}, \hat{S}_{0Vg}, \hat{S}_{0E}$ in the phased antenna array (PAA) mode, we will establish a static spatial (with a spatial frequency H_0) distribution of the following parameters: (a) deviation $\tilde{z}(x) = \tilde{z}_{0\tilde{V}}\cos(H_0 x)$ of the boundary $z = 0$ from $z = 0$ with amplitude $\tilde{z}_{0\tilde{V}}$ in the pattern $\hat{S}_{0\tilde{V}}$ (Section 1, Fig. 1c); (b) deviation $\tilde{z}(x) = \tilde{z}_{0\tilde{V}g}\cos(H_0 x)\exp[-2k_0 y]$ of the boundary from $z = 0$ with amplitude $\tilde{z}_{0\tilde{V}g}$ in the pattern $\hat{S}_{0\tilde{V}g}$ (Section 2, Fig. 2a); (c) charge density $\tilde{\sigma}(x) = \tilde{\sigma}_{0\tilde{E}}\cos(H_0 x)$ with amplitude $\tilde{\sigma}_{0\tilde{E}}$ in the pattern $\hat{S}_{0\tilde{E}}$ (Section 3, Fig. 2c). Then we will set the mode of towing these static structures (a)-(c) along the axis "x" at a constant speed U_0. At the absence of space-time restrictions ($L_0 = \infty$, $T_0 = \infty$) we will get a running sinusoidal along "x" (with frequency $h_0 = H_0$) and along "t" (with frequency $\omega_0 = U_0 H_0$) excitation (with amplitudes $\tilde{z}_{0\tilde{V}}$, $\tilde{z}_{0\tilde{V}g}$, $\tilde{\sigma}_{0\tilde{E}}$) of the boundary $z = 0$ and replacement of patterns $\hat{S}_{0V} \Rightarrow \hat{S}_{0\tilde{V}}$, $\hat{S}_{0Vg} \Rightarrow \hat{S}_{0\tilde{V}g}$, $\hat{S}_{0E} \Rightarrow \hat{S}_{0\tilde{E}}$.

5. General characteristics of patterns in phased array mode and towing mode

Phased array mode. When the boundary $z = 0$ is excited both in a phased antenna array (*i.e.* in patterns $\hat{S}_{0V}$, $\hat{S}_{0Vg}$, $\hat{S}_{0E}$) at spatial h_0 and temporal ω_0 frequencies, the dimensionless complex components of the surface densities of the normal power flux $\overline{W}_{0V}/w_{0V} \sim \mathrm{Re}(\mathbf{z}_0\mathbf{W}_{0V})$, $\overline{W}_{0Vg}/w_{0E} \sim \mathrm{Re}(\mathbf{z}_0\mathbf{W}_{0Vg})$, $\overline{W}_{0E}/w_{0E} \sim \mathrm{Re}(\mathbf{z}_0\mathbf{W}_{0E})$ and

$\overline{\overline{W}}_{0\mathrm{V}}/\mathrm{w}_{0\mathrm{V}} \sim \mathrm{Im}(\mathbf{z}_0\mathbf{W}_{0\mathrm{V}})$, $\overline{\overline{W}}_{0\mathrm{Vg}}/\mathrm{w}_{0\mathrm{E}} \sim \mathrm{Im}(\mathbf{z}_0\mathbf{W}_{0\mathrm{Vg}})$, $\overline{\overline{W}}_{0\mathrm{E}}/\mathrm{w}_{0\mathrm{E}} \sim \mathrm{Im}(\mathbf{z}_0\mathbf{W}_{0\mathrm{E}})$, as well as the tangential force

$$\overline{F}_{0\mathrm{V}}/(\mathrm{w}_{0\mathrm{V}}/c_a) = [\mathrm{Re}(\mathbf{z}_0\mathbf{W}_{0\mathrm{V}})/(\omega_0/h_0)]/(\mathrm{w}_{0\mathrm{V}}/c_a),$$

$$\overline{F}_{0\mathrm{Vg}}/(\mathrm{w}_{0\mathrm{Vg}}/c_\mathrm{g}) = [\mathrm{Re}(\mathbf{z}_0\mathbf{W}_{0\mathrm{Vg}})/(\omega_0/h_0)]/(\mathrm{w}_{0\mathrm{Vg}}/c_\mathrm{g}),$$

$$\overline{F}_{0\mathrm{E}}/(\mathrm{w}_{0\mathrm{E}}/c_e) = [\mathrm{Re}(\mathbf{z}_0\mathbf{W}_{0\mathrm{E}})/(\omega_0/h_0)]/(\mathrm{w}_{0\mathrm{E}}/c_e)$$

and

$$\overline{\overline{F}}_{0\mathrm{V}}/(\mathrm{w}_{0\mathrm{V}}/c_a) = [\mathrm{Im}(\mathbf{z}_0\mathbf{W}_{0\mathrm{V}})/(\omega_0/h_0)]/(\mathrm{w}_{0\mathrm{V}}/c_a),$$

$$\overline{\overline{F}}_{0\mathrm{Vg}}/(\mathrm{w}_{0\mathrm{Vg}}/c_\mathrm{g}) = [\mathrm{Im}(\mathbf{z}_0\mathbf{W}_{0\mathrm{Vg}})/(\omega_0/h_0)]/(\mathrm{w}_{0\mathrm{Vg}}/c_\mathrm{g}),$$

$$\overline{\overline{F}}_{0\mathrm{E}}/(\mathrm{w}_{0\mathrm{E}}/c_e) = [\mathrm{Im}(\mathbf{z}_0\mathbf{W}_{0\mathrm{E}})/(\omega_0/h_0)]/(\mathrm{w}_{0\mathrm{E}}/c_e)$$

(where $\mathrm{w}_{0\mathrm{V}} = |V_{0\mathrm{V}}|^2 \rho_0 c_a/2$, $\mathrm{w}_{0\mathrm{Vg}} = (\rho_0 g_0/2\omega_0)\ \exp[-2k_0 y]\ |V_{0\mathrm{Vg}}|^2$, $\mathrm{w}_{0\mathrm{E}} = |E_{0\mathrm{E}}|^2\sqrt{\varepsilon_0/\mu_0}$ $c_\mathrm{g} = g_0/\omega_0$, see Fig. 3a,b) can be expressed in terms of the values $\overline{G}^{\mathrm{z}}_{0\mathrm{V}}, \overline{\overline{G}}^{\mathrm{z}}_{0\mathrm{V}}$ (see (3)) of the pattern $\hat{\mathrm{S}}_{0\mathrm{V}}$:

$$\overline{W}_{0\mathrm{V}}/\mathrm{w}_{0\mathrm{V}} = \overline{G}^{\mathrm{z}}_{0\mathrm{V}}(h_0/k_0),\ \overline{W}_{0\mathrm{Vg}}/\mathrm{w}_{0\mathrm{Vg}} = \overline{G}^{\mathrm{z}}_{0\mathrm{V}}(h_0/k_0),\ \overline{W}_{0\mathrm{E}}/\mathrm{w}_{0\mathrm{E}} = \overline{G}^{\mathrm{z}}_{0\mathrm{V}}(h_0/k_0), \tag{11}$$

$$\overline{\overline{W}}_{0\mathrm{V}}/\mathrm{w}_{0\mathrm{V}} = \overline{\overline{G}}^{\mathrm{z}}_{0\mathrm{V}}(h_0/k_0),\ \overline{\overline{W}}_{0\mathrm{Vg}}/\mathrm{w}_{0\mathrm{Vg}} = \overline{\overline{G}}^{\mathrm{z}}_{0\mathrm{V}}(h_0/k_0),\ \overline{\overline{W}}_{0\mathrm{E}}/\mathrm{w}_{0\mathrm{E}} = \overline{\overline{G}}^{\mathrm{z}}_{0\mathrm{V}}(h_0/k_0), \tag{12}$$

$$\overline{F}_{0\mathrm{V}}/(\mathrm{w}_{0\mathrm{V}}/c_a) = (h_0/k_0)\ \overline{G}^{\mathrm{z}}_{0\mathrm{V}}(h_0/k_0),\ \overline{\overline{F}}_{0\mathrm{V}}/(\mathrm{w}_{0\mathrm{V}}/c_a) = (h_0/k_0)\ \overline{\overline{G}}^{\mathrm{z}}_{0\mathrm{V}}(h_0/k_0), \tag{13}$$

$$\overline{F}_{0\mathrm{Vg}}/(\mathrm{w}_{0\mathrm{Vg}}/c_\mathrm{g}) = (h_0/k_0)\ \overline{G}^{\mathrm{z}}_{0\mathrm{V}}(h_0/k_0),\ \overline{\overline{F}}_{0\mathrm{Vg}}/(\mathrm{w}_{0\mathrm{Vg}}/c_\mathrm{g}) = (h_0/k_0)\ \overline{\overline{G}}^{\mathrm{z}}_{0\mathrm{V}}(h_0/k_0), \tag{14}$$

$$\overline{F}_{0\mathrm{E}}/(\mathrm{w}_{0\mathrm{E}}/c_e) = (h_0/k_0)\ \overline{G}^{\mathrm{z}}_{0\mathrm{V}}(h_0/k_0),\ \overline{\overline{F}}_{0\tilde{\mathrm{E}}}/(\mathrm{w}_{0\tilde{\mathrm{E}}}/c_e) = (h_0/k_0)\ \overline{\overline{G}}^{\mathrm{z}}_{0\mathrm{V}}(h_0/k_0). \tag{15}$$

Here $\overline{F}_{0\mathrm{V}}, \overline{F}_{0\mathrm{Vg}}, \overline{F}_{0\mathrm{E}}$ are the amplitudes of active ($\sim [1+\cos(2\omega_0 t - 2h_0 x)]$, i.e. with non-zero mean) and $\overline{\overline{F}}_{0\mathrm{V}}, \overline{\overline{F}}_{0\mathrm{Vg}}, \overline{\overline{F}}_{0\mathrm{E}}$ are the amplitudes of reactive ($\sim \sin(2\omega_0 t - 2h_0 x)$, i.e. with zero mean) oscillations of surface power flux densities and tangential force. Based on (11)-(15), we write the dimensionless surface densities (see Fig. 3a,b) of the normal power flux and the tangential reaction force at a point x and at a moment t in the PAA mode:

$$w^{\mathrm{z}}_{0\mathrm{V}}(x,t)/\mathrm{w}_{0\mathrm{V}} = w^{\mathrm{z}}_{0\mathrm{Vg}}(x,t)/\mathrm{w}_{0\mathrm{Vg}} = w^{\mathrm{z}}_{0\mathrm{E}}(x,t)/\mathrm{w}_{0\mathrm{E}} = \Psi, \tag{16}$$

$$\mathrm{f}_{0\mathrm{V}}(x,t)/(\mathrm{w}_{0\mathrm{V}}/c_a) = \mathrm{f}_{0\mathrm{Vg}}(x,t)/(\mathrm{w}_{0\mathrm{Vg}}/c_\mathrm{g}) = \mathrm{f}_{0\mathrm{E}}(x,t)/(\mathrm{w}_{0\mathrm{E}}/c_e) = -(h_0/k_0)\Psi, \tag{17}$$

$$\Psi = \Psi(x,t;\omega_0,h_0,h_0/k_0) = \overline{G}^{\mathrm{z}}_{0\mathrm{V}}(h_0/k_0)\ [1+\cos(2\omega_0 t - 2h_0 x)] + \overline{\overline{G}}^{\mathrm{z}}_{0\mathrm{V}}(h_0/k_0)\ \sin(2\omega_0 t - 2h_0 x). \tag{18}$$

At $|h_0| < k_0$, the reaction force of patterns $\hat{\mathrm{S}}_{0\mathrm{V}}$, $\hat{\mathrm{S}}_{0\mathrm{Vg}}$, $\hat{\mathrm{S}}_{0\mathrm{E}}$ contains a constant (along "x" and "t") component, which can be interpreted, for example, as the force of the wave thrust of a vibrational vehicle [17]. If instead $\Phi_0 = \exp(i\omega_0 t - ih_0 x)$ we apply excitation $\Phi_1 = \cos(\omega_0 t)\cos(h_0 x)$, then the projection of the power flow on the directions $\mathbf{x}_0$ and $-\mathbf{x}_0$ will be the same, and the force of the wave thrust of such a pattern will become equal to zero.

Towing mode. On the other hand, when the boundary $z = 0$ is excited by towing at the speed U_0 of the static structure (*i.e.*, in the patterns $\hat{\mathrm{S}}_{0\tilde{\mathrm{V}}}$, $\hat{\mathrm{S}}_{0\tilde{\mathrm{V}}\mathrm{g}}$, $\hat{\mathrm{S}}_{0\tilde{\mathrm{E}}}$, sections 4.1.1, 4.1.2, 4.1.3, 4.2) with a spatial frequency H_0, the dimensionless surface densities of the normal power flux $\overline{W}_{0\tilde{\mathrm{V}}}/\mathrm{w}_{0\tilde{\mathrm{V}}}$, $\overline{W}_{0\tilde{\mathrm{V}}\mathrm{g}}/\mathrm{w}_{0\tilde{\mathrm{V}}\mathrm{g}}$, $\overline{W}_{0\tilde{\mathrm{E}}}/\mathrm{w}_{0\tilde{\mathrm{E}}}$ and $\overline{\overline{W}}_{0\tilde{\mathrm{V}}}/\mathrm{w}_{0\tilde{\mathrm{V}}}$, $\overline{\overline{W}}_{0\tilde{\mathrm{V}}\mathrm{g}}/\mathrm{w}_{0\tilde{\mathrm{V}}\mathrm{g}}$, $\overline{\overline{W}}_{0\tilde{\mathrm{E}}}/\mathrm{w}_{0\tilde{\mathrm{E}}}$, as well as the tangential force $\overline{F}_{0\tilde{\mathrm{V}}}/(\mathrm{w}_{0\tilde{\mathrm{V}}}/c_a)$, $\overline{F}_{0\tilde{\mathrm{V}}\mathrm{g}}/(\mathrm{w}_{0\tilde{\mathrm{V}}\mathrm{g}}/c_\mathrm{g})$, $\overline{F}_{0\tilde{\mathrm{E}}}/(\mathrm{w}_{0\tilde{\mathrm{E}}}/c_e)$ and $\overline{\overline{F}}_{0\tilde{\mathrm{V}}}/(\mathrm{w}_{0\tilde{\mathrm{V}}}/c_a)$, $\overline{\overline{F}}_{0\tilde{\mathrm{V}}\mathrm{g}}/(\mathrm{w}_{0\tilde{\mathrm{V}}\mathrm{g}}/c_\mathrm{g})$, $\overline{\overline{F}}_{0\tilde{\mathrm{E}}}/(\mathrm{w}_{0\tilde{\mathrm{E}}}/c_e)$ have the following form:

$$\overline{W}_{0\tilde{\mathrm{V}}}/\mathrm{w}_{0\tilde{\mathrm{V}}}=\overline{G}^{\mathrm{z}}_{0\mathrm{V}}(c_a/U_0),\ \ \overline{W}_{0\tilde{\mathrm{V}}\mathrm{g}}/\mathrm{w}_{0\tilde{\mathrm{V}}\mathrm{g}}=\overline{G}^{\mathrm{z}}_{0\mathrm{V}}(c_g/U_0),\ \ \overline{W}_{0\tilde{\mathrm{E}}}/\mathrm{w}_{0\tilde{\mathrm{E}}}=\overline{G}^{\mathrm{z}}_{0\mathrm{V}}(c_e/U_0), \tag{19}$$

$$\overline{\overline{W}}_{0\tilde{\mathrm{V}}}/\mathrm{w}_{0\tilde{\mathrm{V}}}=\overline{\overline{G}}^{\mathrm{z}}_{0\mathrm{V}}(c_a/U_0),\ \ \overline{\overline{W}}_{0\tilde{\mathrm{V}}\mathrm{g}}/\mathrm{w}_{0\tilde{\mathrm{V}}\mathrm{g}}=\overline{\overline{G}}^{\mathrm{z}}_{0\mathrm{V}}(c_g/U_0),\ \ \overline{\overline{W}}_{0\tilde{\mathrm{E}}}/\mathrm{w}_{0\tilde{\mathrm{E}}}=\overline{\overline{G}}^{\mathrm{z}}_{0\mathrm{V}}(c_e/U_0), \tag{20}$$

$$\overline{F}_{0\tilde{\mathrm{V}}}/(\mathrm{w}_{0\tilde{\mathrm{V}}}/c_a)=(c_a/U_0)\ \overline{G}^{\mathrm{z}}_{0\mathrm{V}}(c_a/U_0),\ \ \overline{\overline{F}}_{0\tilde{\mathrm{V}}}/(\mathrm{w}_{0\tilde{\mathrm{V}}}/c_a)=(c_a/U_0)\ \overline{\overline{G}}^{\mathrm{z}}_{0\mathrm{V}}(c_a/U_0), \tag{21}$$

$$\overline{F}_{0\tilde{\mathrm{V}}\mathrm{g}}/(\mathrm{w}_{0\tilde{\mathrm{V}}\mathrm{g}}/c_g)=(c_g/U_0)\ \overline{G}^{\mathrm{z}}_{0\mathrm{V}}(c_g/U_0),\ \ \overline{\overline{F}}_{0\tilde{\mathrm{V}}\mathrm{g}}/(\mathrm{w}_{0\tilde{\mathrm{V}}\mathrm{g}}/c_g)=(c_g/U_0)\ \overline{\overline{G}}^{\mathrm{z}}_{0\mathrm{V}}(c_g/U_0), \tag{22}$$

$$\overline{F}_{0\tilde{\mathrm{E}}}/(\mathrm{w}_{0\tilde{\mathrm{E}}}/c_e)=(c_e/U_0)\ \overline{G}^{\mathrm{z}}_{0\mathrm{V}}(c_e/U_0),\ \ \overline{\overline{F}}_{0\tilde{\mathrm{E}}}/(\mathrm{w}_{0\tilde{\mathrm{E}}}/c_e)=(c_e/U_0)\ \overline{\overline{G}}^{\mathrm{z}}_{0\mathrm{V}}(c_e/U_0). \tag{23}$$

Here $\overline{F}_{0\tilde{\mathrm{V}}}$, $\overline{F}_{0\tilde{\mathrm{V}}\mathrm{g}}$, $\overline{F}_{0\tilde{\mathrm{E}}}$ are the amplitudes of active ($\sim[1+\cos(2\omega_0 t-2h_0 x)]$, with non-zero mean, $\omega_0=H_0U_0$, $h_0=H_0$) and $\overline{\overline{F}}_{0\tilde{\mathrm{V}}}, \overline{\overline{F}}_{0\tilde{\mathrm{V}}\mathrm{g}}, \overline{\overline{F}}_{0\tilde{\mathrm{E}}}$ reactive ($\sim\sin(2\omega_0 t-2h_0 x)$, with zero mean) fluctuations of the surface power flux densities and tangential force corresponding to the forces of patterns $\hat{\mathrm{S}}_{0\mathrm{V}}$, $\hat{\mathrm{S}}_{0\mathrm{V}\mathrm{g}}$, $\hat{\mathrm{S}}_{0\mathrm{E}}$ ($\omega_0=H_0U_0$, $h_0=H_0$), but with amplitudes of boundary excitation which are taken from patterns $\hat{\mathrm{S}}_{0\tilde{\mathrm{V}}}$, $\hat{\mathrm{S}}_{0\tilde{\mathrm{V}}\mathrm{g}}$, $\hat{\mathrm{S}}_{0\tilde{\mathrm{E}}}$ (i.e. at $U_0\neq 0$). Further, $\mathrm{w}_{0\tilde{\mathrm{V}}}=\overline{W}_{0\mathrm{V}}(h_0=0)$, $\mathrm{w}_{0\tilde{\mathrm{V}}\mathrm{g}}=\overline{W}_{0\mathrm{V}\mathrm{g}}(h_0=0)$, $\mathrm{w}_{0\tilde{\mathrm{E}}}=\overline{W}_{0\mathrm{E}}(h_0=0)$ are the surface densities of normal active power flows corresponding to the power flows of patterns $\hat{\mathrm{S}}_{0\mathrm{V}}$, $\hat{\mathrm{S}}_{0\mathrm{V}\mathrm{g}}$, $\hat{\mathrm{S}}_{0\mathrm{E}}$, but at $h_0=0$ and with boundary excitation amplitudes which are taken from patterns $\hat{\mathrm{S}}_{0\tilde{\mathrm{V}}}$, $\hat{\mathrm{S}}_{0\tilde{\mathrm{V}}\mathrm{g}}$, $\hat{\mathrm{S}}_{0\tilde{\mathrm{E}}}$ (i.e. at $U_0\neq 0$); c_a, $c_g=g_0/\omega_0=g_0/H_0U_0$, c_e are the phase velocities of sound, gravitational (on water), and electromagnetic waves, respectively. Based on (19)-(23), we write the universal dimensionless surface densities (see Fig. 3a,b) of the normal power flow and the tangential reaction force at the point x and t at the moment in the towing mode:

$$w^{\mathrm{z}}_{0\tilde{\mathrm{V}}}(x,t)/\tilde{\mathrm{w}}_{0\tilde{\mathrm{V}}}=(\Psi)_{c_0=c_a},\ \ \mathrm{f}_{0\tilde{\mathrm{V}}}(x,t)/(\tilde{\mathrm{w}}_{0\tilde{\mathrm{V}}}/c_a)=-(c_a/U_0)\ (\Psi)_{c_0=c_a}, \tag{24}$$

$$w^{\mathrm{z}}_{0\tilde{\mathrm{V}}\mathrm{g}}(x,t)/\tilde{\mathrm{w}}_{0\tilde{\mathrm{V}}\mathrm{g}}=(\Psi)_{c_0=c_g},\ \ \mathrm{f}_{0\tilde{\mathrm{V}}\mathrm{g}}(x,t)/(\tilde{\mathrm{w}}_{0\tilde{\mathrm{V}}\mathrm{g}}/c_g)=-(c_g/U_0)\ (\Psi)_{c_0=c_g}, \tag{25}$$

$$w^{\mathrm{z}}_{0\tilde{\mathrm{E}}}(x,t)/\tilde{\mathrm{w}}_{0\tilde{\mathrm{E}}}=(\Psi)_{c_0=c_e},\ \ \mathrm{f}_{0\tilde{\mathrm{E}}}(x,t)/(\tilde{\mathrm{w}}_{0\tilde{\mathrm{E}}}/c_e)=-(c_e/U_0)\ (\Psi)_{c_0=c_e}, \tag{26}$$

$$\Psi=\Psi(x,t;U_0H_0,H_0,c_0/U_0)=\overline{G}^{\mathrm{z}}_{0\mathrm{V}}(c_0/U_0)\ [1+\cos(2U_0H_0t-2H_0x)]+\overline{\overline{G}}^{\mathrm{z}}_{0\mathrm{V}}(c_0/U_0)\ \sin(2U_0H_0t-2H_0x). \tag{27}$$

Here $\tilde{\mathrm{w}}_{0\tilde{\mathrm{V}}}=(1/2)\rho_0 c_{0a}H_0^2U_0^2\left|\tilde{z}_{0\tilde{\mathrm{V}}}\right|^2$, $\tilde{\mathrm{w}}_{0\tilde{\mathrm{V}}\mathrm{g}}(y)=(1/2)\rho_0 g_0 H_0U_0\left|\tilde{z}_{0\tilde{\mathrm{V}}}\right|^2\exp[-2H_0^2U_0^2y/g_0]$, $\tilde{\mathrm{w}}_{0\tilde{\mathrm{E}}}=\left|E_{0\mathrm{E}}\right|^2\sqrt{\varepsilon_0/\mu_0}$ are the surface densities of normal power fluxes at the boundary $z=0$ in patterns $\hat{\mathrm{S}}_{0\mathrm{V}}$, $\hat{\mathrm{S}}_{0\mathrm{V}\mathrm{g}}$, $\hat{\mathrm{S}}_{0\mathrm{E}}$ at $h_0=0$, $\omega_0=U_0H_0$ with amplitudes $V_{0\tilde{\mathrm{V}}}=\tilde{z}_{0\tilde{\mathrm{V}}}H_0U_0$, $V_{0\tilde{\mathrm{V}}\mathrm{g}}=\tilde{z}_{0\tilde{\mathrm{V}}\mathrm{g}}H_0U_0\exp[-H_0^2U_0^2y/g_0]$ of normal velocity, and amplitude $\tilde{\sigma}_{0\tilde{\mathrm{E}}}=-2\varepsilon_0E_{0\tilde{\mathrm{E}}}\ (c_e/U_0)\left\{\left[1-(c_e/U_0)^2\right]^{-1/2}\mathbf{I}[U_0-c_e]-i\left[(c_e/U_0)^2-1\right]^{-1/2}\mathbf{I}[c_e-U_0]\right\}$ of charge distribution $\tilde{\sigma}(x)=\tilde{\sigma}_{0\tilde{\mathrm{E}}}\cos(H_0x)$, respectively. The value $\tilde{\sigma}_{0\tilde{\mathrm{E}}}$ determines such a current density $J_{0\tilde{\mathrm{E}}}=U_0\sigma_{0\tilde{\mathrm{E}}}$ that ensures the constancy of the given amplitude $E_{0\tilde{\mathrm{E}}}$ of the tangential electric field at the pattern boundary $z=0$ for any H_0 and U_0 (note that the mechanical rigid corrugated profile in the patterns does not create field energy in the medium, but the static charge distribution at the boundary in the pattern $\hat{\mathrm{S}}_{0\tilde{\mathrm{E}}}$ creates a finite density of electrostatic energy even at $U_0=0$). Since the radiation in this case is generated by the towing of the distributions described above (analogues of this problem were considered briefly in [18], [19], but without the tangential force), the time-constant tangential force that arises in this case is the wave resistance force. The wave drag in the pattern $\hat{\mathrm{S}}_{0\tilde{\mathrm{V}}}$ can be considered as an analog of the "wave crisis" in aerodynamics [20] (an increase in shaking as the aircraft speeds up and then a loss of aircraft speed at

$0 < (U_0 - c_a)/c_a << 1$ due to powerful wave resistance. In the pattern $\hat{S}_{0\tilde{V}g}$, the tangential force considered here is an analog of the wave drag force of a thin boat [21] or, on the contrary, it is analogous to the wave deceleration of a flow flowing around a rigid motionless vertical horizontally corrugated wall near ($0 < (U_0 - U_0^*)/U_0^* << 1$) "resonant velocity" $U_0 = U_0^* = \sqrt{g_0/H_0}$. Towing radiation occurs only at $U_0 > c_a, c_g, c_e$ (see Fig. 3c), and the patterns $\hat{S}_{0\tilde{V}}$, $\hat{S}_{0\tilde{V}g}$, $\hat{S}_{0\tilde{E}}$ can also serve as an illustration of the Vavilov & Cherenkov effect [22]. The towing of the spatial distribution of the electric charge with the speed U_0 at $0 < (U_0 - c_e)/c_e << 1$ in vacuum may raise doubts, but it should be remembered that we are talking about a sinusoidal distribution of charge as a certain continuous medium with a zero-mass density (i.e., without concretization by a discrete set of charged particles).

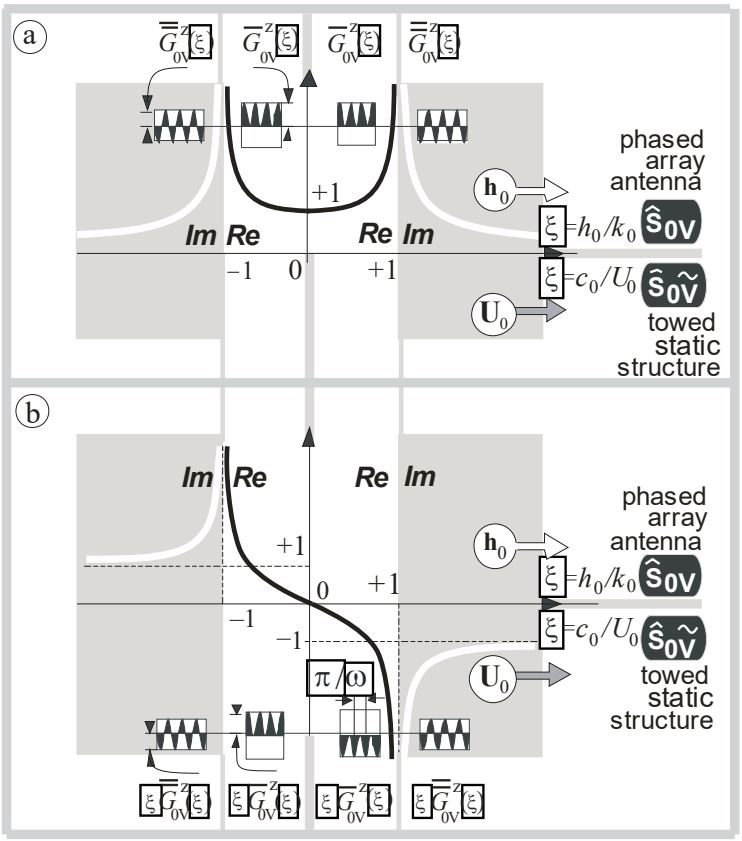

Figure 3. Dimensionless oscillation amplitudes (at the frequency $\omega = 2\omega_0$ (PAA) and $\omega = 2H_0U_0$ (TM) of the surface power flux density $\overline{G}^z_{0V}(\xi)$, $\overline{\overline{G}}^z_{0V}(\xi)$ (a) and the surface density of the tangential force $\xi\overline{G}^z_{0V}(\xi)$, $\xi\overline{\overline{G}}^z_{0V}(\xi)$ (b) when excited in the PAR mode ($\hat{S}_{0V}, \hat{S}_{0Vg}, \hat{S}_{0E}, \xi = h_0/k_0$) and in the towing mode TM ($\hat{S}_{0\tilde{V}}, \hat{S}_{0\tilde{V}g}, \hat{S}_{0\tilde{E}}, \xi = c_0/U_0$, $c_0 = c_a, c_g, c_e$) static structure as a function of $\xi = h_0/k_0$ and $\xi = c_0/U_0$. The gray background in (a, b) indicates the areas $|h_0/k_0|, |c_0/U_0| > 1$ without radiation, corresponding to fluctuations in the power flux and tangential force with zero mean. In addition to oscillations, in the regions $|h_0/k_0|, |c_0/U_0| < 1$ there is also a constant and non-zero radiation power flux, wave thrust (in the phased array mode) or wave resistance (in the towing mode).

6. Geometric deviations of the acoustic pattern $\hat{S}_{0V}$

Below, we consider the emission of acoustic patterns with a given excitation (1) of normal vibrational velocity, but differing from a flat pattern $\hat{S}_{0V}$ either in finite dimension $|x| \le L_0 < \infty$ or in a finite radius $R_0 < \infty$ of surface curvature.

6.1. Finite dimension of the flat acoustical pattern $\hat{S}_{1V}$

Let a two-dimensional distribution of normal vibrational velocity be given in a pattern $\hat{S}_{1V}$ on a strip $-L_0 < x < L_0 < \infty$ (between two half-infinite rigid planes, *i.e.* $|x| > L_0$), where is the excitation amplitude of the pattern in the PAA mode. Due to the linearity of the boundary value problem, we can represent the sound pressure $p(x,z,t)$ created by the pattern $\hat{S}_{1V}$ as the sum of the pressures created by each of the frequencies $-\infty < h < \infty$ of the Fourier spectrum (along "x") $V_{1V} 2L_0 \{(\sin[(h-h_0)L])/(h-h_0)L\} \exp(i\omega_0 t)$ of the velocity distribution $\upsilon_z(x,0,t)$ at the boundary $z = 0$. The patterns $\hat{S}_{0V}$, $\hat{S}_{0P}$, $\hat{S}_{0Vg}$, $\hat{S}_{0Pg}$, $\hat{S}_{0J}$, $\hat{S}_{0E}$ had a directivity diagram in the form of a delta function $\sim \delta(\theta - \alpha)$ of the viewing angle θ, where $\alpha = \arccos(h_0 / k_0)$, and for the pattern $\hat{S}_{1V}$, the direction of maximum power and the width of the main lobe depend on the wave dimension $k_0 L_0$ of the pattern and on the dimensionless spatial excitation frequency h_0 / k_0. The radiation directivity $\Xi_{1V}(\vartheta; h_0, k_0, L_0) = |p(R\cos(\vartheta), R\sin(\vartheta); h_0, k_0, L_0)|^2 / |p(0,R;0,k_0,L_0)|^2$ (at the observation direction ϑ) of the pattern $\hat{S}_{1V}$ is defined as the square of the acoustic pressure modulus at the observation point $\{x = R\cos(\vartheta),\ z = R\sin(\vartheta)\}$ at $R >> k_0 L_0^2$, normalized by the square of the pressure modulus at the point $x = 0$, $z = R$, $\vartheta = \pi/2$ at $h_0 = 0$. For the pattern $\hat{S}_{1V}$, the dimensionless radiation resistance (analog of $\overline{G}_{0V}^{z}$) is equal to

$$\overline{G}_{1V} == \int_0^{\pi} \Xi_{1V}(\vartheta; h_0, k_0, L_0) d\vartheta \Big/ \int_0^{\pi} \Xi_{1V}(\vartheta; 0, k_0, L_0) d\vartheta \quad \text{or}$$

$$\overline{G}_{0V} = \left[\int_{-\infty}^{\infty} \mathrm{Re}(p(x,0,t;h_0) * \upsilon_z(x,0,t;h_0) dx\right] \Big/ \left[\int_{-\infty}^{\infty} \mathrm{Re}(p(x,0,t;0) * \upsilon_z(x,0,t;0) dx\right].$$

The power $\overline{\overline{G}}_{1V}$ of the reactive field of the pattern $\hat{S}_{1V}$ is

$$\overline{\overline{G}}_{0V} = \left[\int_{-\infty}^{\infty} \mathrm{Im}(p(x,0,t;h_0) * \upsilon_z(x,0,t;h_0) dx\right] \Big/ \left[\int_{-\infty}^{\infty} \mathrm{Re}(p(x,0,t;0) * \upsilon_z(x,0,t;0) dx\right].$$

On Fig. 4a,b shows that at $L_0 k_0 \to \infty$ the characteristic $\overline{G}_{1V}$ tends to $\overline{G}_{0V}^{z}$, always remaining less than it, i.e. $\overline{G}_{1V}(L_0 k_0 \to \infty) \to \overline{G}_{0V}^{z} > \overline{G}_{1V}$ (the same $\overline{\overline{G}}_{1V}(L_0 k_0 \to \infty) \to \overline{\overline{G}}_{0V}^{z}$ for the imaginary part $\overline{\overline{G}}_{1V}$, but with a slight difference: $\overline{\overline{G}}_{0V}^{z} < \overline{\overline{G}}_{1V}$). On fig. 4c, d, e shows the evolution of the main lobe of the directivity diagram Ξ_{1V} of pattern $\hat{S}_{1V}$ and shows that at $h_0 \to k_0$ the main lobe of the directivity diagram expands, and the maximum $g_{1V} = \max_{h_0}\left[\overline{G}_{1V}\right]$ of the function $\overline{G}_{1V}$ (Fig. 4a) is closing to the expression $g_{1V} \approx \sqrt{L_0 k_0}$. Let us comment qualitatively on this numerical fact. Let, within the main lobe, the field value does not depend on the angle (and outside it, the field is equal to zero), and within the main lobe, the fields created by all elements of the pattern add up in phase. Let us consider the in-phase addition of element fields of $\hat{S}_{1V}$ in two cases: (a) at the observation direction $\vartheta_1 = \pi/2$ (at $h_0 = 0$) with the width $\delta_1 \approx (k_0 L_0)^{-1}$ of the main lobe and its amplitude A; (b) at the observation direction $\vartheta_2 = 0$ (at $h_0 \approx k_0$) with the width $\delta_2 \approx (k_0 L_0)^{-1/2}$ of the main lobe and with the same amplitude A. Now it is easy to see that with an increase $L_0 k_0$, the value g_{1V} grows as $\delta_2 / \delta_1 \approx \sqrt{L_0 k_0}$.

6.2 Finite curvature of acoustical patterns

In this section, we will consider the influence of the curvature of the pattern boundary on the power flux density from the pattern surface during excitation in the PAA mode). Below, as a model for curvilinear patterns, we will consider a

circular cylinder of infinite length $L_0 = \infty$ and of finite radius $R_0 < \infty$ with an axis $\mathbf{x}_0$ in two versions: with a phase running along the azimuth of the cylinder (the azimuthal phasor $\mathbf{h}_0 \uparrow\uparrow \mathbf{Q}_0$ of the pattern $\hat{\mathrm{S}}_{2\mathrm{V}}$, where $\mathbf{Q}_0$ the azimuthal unit vector is on the surface of the cylinder, $|\mathbf{Q}_0| = 1$), and with a phase running along the axis (axial phasor $\mathbf{h}_0 \uparrow\uparrow \mathbf{x}_0$).

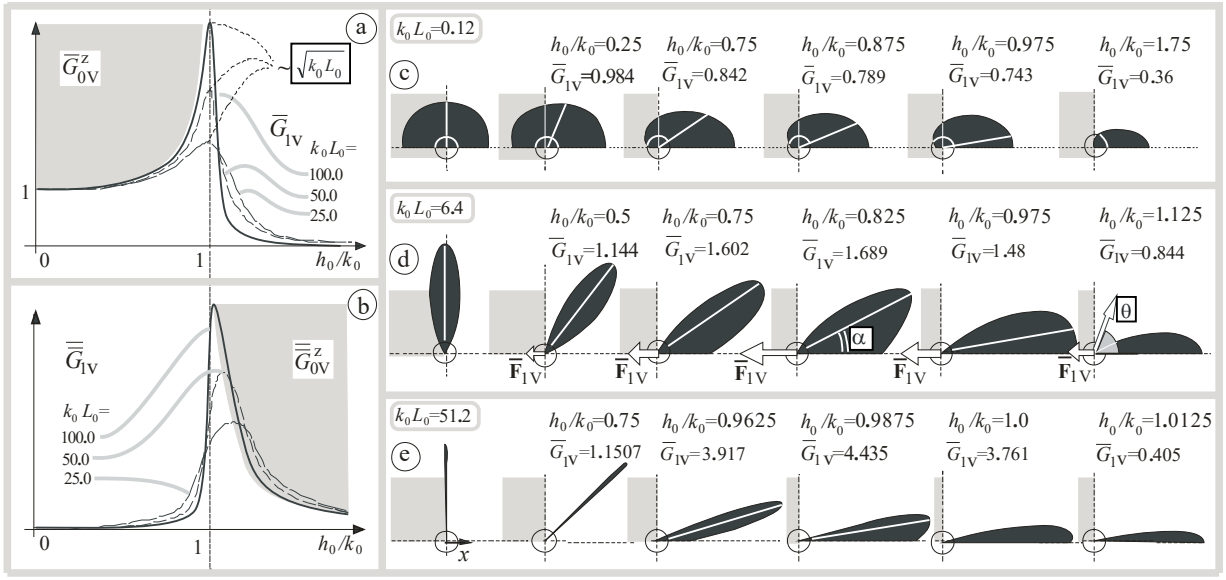

Figure 4. Characteristics of the finite flat pattern $\hat{\mathrm{S}}_{1\mathrm{V}}$: (a) $\overline{G}_{1\mathrm{V}}$ —total active radiation power of the pattern normalized to the same value at $h_0 = 0$; (b) $\overline{\overline{G}}_{1\mathrm{V}}$ is the total reactive power of the field on the surface of the pattern $\hat{\mathrm{S}}_{1\mathrm{V}}$, normalized to the total active power at $h_0 = 0$, the boundaries of the shaded areas correspond to the characteristics $\overline{G}^{z}_{0\mathrm{V}}$ and $\overline{\overline{G}}^{z}_{0\mathrm{V}}$ of the pattern $\hat{\mathrm{S}}_{0\mathrm{V}}$; (c), (d), (e) changes in the main lobe of the radiation of the pattern $\hat{\mathrm{S}}_{1\mathrm{V}}$ in terms of power (normalized to the maximum of the radiation of pattern $\hat{\mathrm{S}}_{1\mathrm{V}}$ at $h_0 = 0$) due to variations in the parameters h_0 / k_0 and $k_0 L_0$. $\overline{\mathrm{F}}_{1\mathrm{V}}$ is the force of the wave thrust of the pattern $\hat{\mathrm{S}}_{1\mathrm{V}}$.

6.2.1. Cylindrical pattern $\hat{\mathrm{S}}_{2\mathrm{V}}$ with azimuthal phasor

For the wave potential $\varphi_{2\mathrm{V}}(r,\vartheta,t)$ ($r \geq R_0$, $0 \leq \vartheta < 2\pi$, $|x| < L_0 = \infty$, $\partial / \partial x = 0$), satisfying the cylindrical wave equation, in this problem (see Fig. 5a) with the boundary condition $-\{(\partial / \partial r)\varphi_{2\mathrm{V}}(r,\vartheta,t)\}_{r=R_0} = V_{2\mathrm{V}} \exp(i\omega_0 t - ih_0 R_0 \vartheta)$ ($V_{2\mathrm{V}}$ is the normal velocity amplitude, $h_0 / k_0 = \mathrm{n} / k_0 R_0$, $n = 0,1,2...$) we obtain the radiation parameters of the pattern $\hat{\mathrm{S}}_{2\mathrm{V}}$:

$$\overline{G}^{\mathrm{r}}_{2\mathrm{V}}(\mathrm{n}/k_0 R_0) = \frac{\mathrm{Re}[(p_{2\mathrm{V}}(\mathrm{n})) * (\upsilon_{2\mathrm{V}}(\mathrm{n}))_{\mathrm{r}}]}{\mathrm{Re}[(p_{2\mathrm{V}}(0)) * (\upsilon_{2\mathrm{V}}(0))_{\mathrm{r}}]}, \quad \overline{G}^{\mathrm{r}}_{2\mathrm{V}}(\mathrm{n}/k_0 R_0) = \frac{\mathrm{Re}[(p_{2\mathrm{V}}(\mathrm{n})) * (\upsilon_{2\mathrm{V}}(\mathrm{n}))_{\mathrm{r}}]}{\mathrm{Re}[(p_{2\mathrm{V}}(0)) * (\upsilon_{2\mathrm{V}}(0))_{\mathrm{r}}]}.$$

Taking into account the expressions $(\upsilon_{2\mathrm{V}})_{\mathrm{r}} = -(\partial / \partial r)\varphi_{2\mathrm{V}}$, $p_{2\mathrm{V}} = \rho_0 (\partial / \partial t)\varphi_{2\mathrm{V}}$, we obtain (similarly to (3) $\overline{G}^{z}_{0\mathrm{V}}$, $\overline{\overline{G}}^{z}_{0\mathrm{V}}$):

$$\overline{G}^{\mathrm{r}}_{2\mathrm{V}}(\mathrm{n}/k_0 R_0) = \frac{\mathrm{Re}[i(\mathrm{H}^{(2)}_{\mathrm{n}}(\xi)) / (\mathrm{H}^{(2)}_{\mathrm{n}}(\xi))'_{\xi}]_{\xi = k_0 R_0}}{\mathrm{Re}[i(\mathrm{H}^{(2)}_{0}(\xi)) / (\mathrm{H}^{(2)}_{0}(\xi))'_{\xi}]_{\xi = k_0 R_0}}, \quad \overline{\overline{G}}^{\mathrm{r}}_{2\mathrm{V}}(\mathrm{n}/k_0 R_0) = \frac{\mathrm{Im}[i(\mathrm{H}^{(2)}_{\mathrm{n}}(\xi)) / (\mathrm{H}^{(2)}_{\mathrm{n}}(\xi))'_{\xi}]_{\xi = k_0 R_0}}{\mathrm{Re}[i(\mathrm{H}^{(2)}_{0}(\xi)) / (\mathrm{H}^{(2)}_{0}(\xi))'_{\xi}]_{\xi = k_0 R_0}},$$

where $\mathrm{H}^{(2)}_{\mathrm{n}}(\xi)$ is the Hankel function of the second kind of the n -th order. On Fig. 5b, only discrete points

$h_0 / k_0 = \mathrm{n}/k_0 R_0$ have physical sense and are used as interpolation nodes. As $k_0 R_0$ increases, function $\overline{G}^{\mathrm{r}}_{2\mathrm{V}}(h_0 / k_0)$ becomes closer to $\overline{G}^{\mathrm{z}}_{0\mathrm{V}}(h_0 / k_0)$, but this closing becomes more and more slow, as well as the growth of the maxima $g_2(k_0 R_0) = \max\limits_{h_0}\left[\overline{G}^{\mathrm{r}}_{2\mathrm{V}}(h_0 / k_0)\right]$ (Fig. 5c). On the surface, the slope angle of the power flow lines is $\alpha = \arccos(h_0 / k_0)$, and in the far zone (i.e., at distance $>> R_0^2 k_0$) they become radial (Fig. 5a), i.e. there is no directivity of the radiation, in contrast to the pattern $\hat{\mathrm{S}}_{0\mathrm{V}}$.

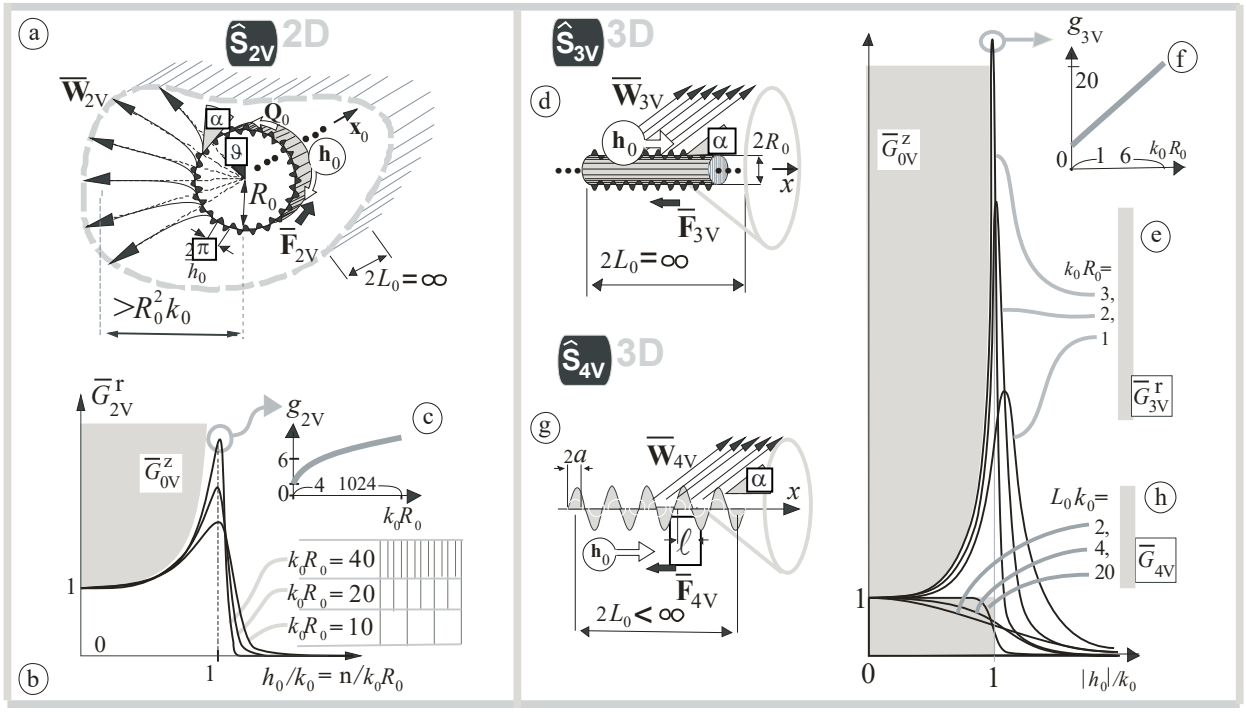

Figure 5. Cylindrical pattern $\hat{\mathrm{S}}_{2\mathrm{V}}$ with azimuthal phasor: (a) pattern $\hat{\mathrm{S}}_{2\mathrm{V}}$ geometry; (b) normal (and normalized) surface radiation power flux density $\overline{G}^{\mathrm{r}}_{2\mathrm{V}}$; (c) dependence of the function $\overline{G}^{\mathrm{z}}_{2\mathrm{V}}$ maximum $g_{2\mathrm{V}}$ on the wave dimension $k_0 R_0$ of the cylinder cross section. Cylindrical pattern $\hat{\mathrm{S}}_{3\mathrm{V}}$ with axial phasor: (d) pattern $\hat{\mathrm{S}}_{3\mathrm{V}}$ geometry; (e) normalized surface radiation power flux density $\overline{G}^{\mathrm{r}}_{3\mathrm{V}}$; (f) dependence of the function $\overline{G}^{\mathrm{z}}_{3\mathrm{V}}$ maximum $g_{3\mathrm{V}}$ on the wave dimension $k_0 R_0$ of the cylinder cross section. A pattern $\hat{\mathrm{S}}_{4\mathrm{V}}$ in the form of an equidistant (period ℓ) chain (length $2L_0$) pulsating spheres with given velocity amplitudes and running phases of pulsations: (g) pattern $\hat{\mathrm{S}}_{4\mathrm{V}}$ geometry; (h) normalized total radiated power $\overline{G}_{4\mathrm{V}}$ of the pattern $\hat{\mathrm{S}}_{4\mathrm{V}}$. The borders of the shaded areas correspond to the characteristic and pattern $\hat{\mathrm{S}}_{0\mathrm{V}}$. $\overline{\mathbf{F}}_{2\mathrm{V}}$, $\overline{\mathbf{F}}_{2\mathrm{V}}$, $\overline{\mathbf{F}}_{2\mathrm{V}}$ are the wave thrust forces of the patterns $\hat{\mathrm{S}}_{2\mathrm{V}}$, $\hat{\mathrm{S}}_{3\mathrm{V}}$, $\hat{\mathrm{S}}_{4\mathrm{V}}$.

6.2.2. Cylindrical pattern $\hat{\mathrm{S}}_{3\mathrm{V}}$ with axial phasor

For the wave potential $\varphi_{3\mathrm{V}}(r,x,t)$ ($r \geq R_0$, $-\infty < x < +\infty$, $\partial / \partial \vartheta = 0$), which satisfies the cylindrical wave equation with the boundary condition $-\{(\partial/\partial r)\varphi_{2\mathrm{V}}(r,x,t)\}_{r=R_0} = V_{3\mathrm{V}} \exp(i\omega_0 t - ih_0 x)$ (where $V_{3\mathrm{V}}$ is the amplitude of the normal velocity) of the pattern $\hat{\mathrm{S}}_{3\mathrm{V}}$, with an axial phasor $\mathbf{h}_0 \uparrow\uparrow \mathbf{x}_0$ (see the energy output of the pattern $\hat{\mathrm{S}}_{3\mathrm{V}}$: Fig. 5d). Similarly to the values $\overline{G}^{\mathrm{z}}_{2\mathrm{V}}$, $\overline{\overline{G}}^{\mathrm{z}}_{2\mathrm{V}}$ we obtain for the following energy parameters $\overline{G}^{\mathrm{r}}_{3\mathrm{V}}$ and $\overline{\overline{G}}^{\mathrm{r}}_{3\mathrm{V}}$:

$$\overline{G}^{\mathrm{r}}_{3\mathrm{V}}(h_0/k_0)=\mathrm{Re}\left[i\left(\mathrm{H}^{(2)}_0(\xi)\right)\Big/\left(\mathrm{H}^{(2)}_0(\xi)\right)'_{\xi}\right]_{\xi=k_0R_0\sqrt{1-(h_0/k_0)^2}}\Big/\ \mathrm{Re}\left[i\sqrt{1-(h_0/k_0)^2}\left(\mathrm{H}^{(2)}_0(\xi)\right)\Big/\left(\mathrm{H}^{(2)}_0(\xi)\right)'_{\xi}\right]_{\xi=k_0R_0},$$

$$\overline{\overline{G}}^{\mathrm{r}}_{3\mathrm{V}}(h_0/k_0)=\mathrm{Im}\left[i\left(\mathrm{H}^{(2)}_0(\xi)\right)\Big/\left(\mathrm{H}^{(2)}_0(\xi)\right)'_{\xi}\right]_{\xi=k_0R_0\sqrt{1-(h_0/k_0)^2}}\Big/\ \mathrm{Re}\left[i\sqrt{1-(h_0/k_0)^2}\left(\mathrm{H}^{(2)}_0(\xi)\right)\Big/\left(\mathrm{H}^{(2)}_0(\xi)\right)'_{\xi}\right]_{\xi=k_0R_0}.$$

On fig. 5e,f shows the functions $\overline{G}^{\mathrm{r}}_{3\mathrm{V}}(h_0/k_0)$ and $g_3(k_0R_0)=\max\limits_{h_0}\left[\overline{G}^{\mathrm{r}}_{3\mathrm{V}}(h_0/k_0)\right]$. From Fig. 5d it can be seen that $\overline{G}^{\mathrm{r}}_{3\mathrm{V}}(h_0/k_0)$ approaches to $\overline{G}^{\mathrm{z}}_{0\mathrm{V}}(h_0/k_0)$ with increasing k_0R_0, but faster than $\overline{G}^{\mathrm{r}}_{2\mathrm{V}}(h_0/k_0)$. To better understand the properties of the pattern $\hat{\mathrm{S}}_{3\mathrm{V}}$, for comparison with it, consider the pattern $\hat{\mathrm{S}}_{4\mathrm{V}}$ (Fig. 5g) in the form of a chain $2\mathrm{N}+1$ (with a finite total length $2L_0<\infty$) of pulsating spheres with a diameter $2a$ ($k_0a<<1$), equidistantly (with a period $\ell=L_0/\mathrm{N}>>a$, $\ell<\pi/k_0$) placed on the axis "x" with a linear phase increment $\exp(-ih_0\ell)$ over the period ℓ, t .e. traditional traveling wave antenna [7]. Let us define for the pattern $\hat{\mathrm{S}}_{4\mathrm{V}}$ an analog $\overline{G}_{4\mathrm{V}}=\int_0^{\pi}\Phi_{4\mathrm{V}}(\vartheta;h_0,\omega_0)\sin(\vartheta)\ d\vartheta\Big/\int_0^{\pi}\Phi_{4\mathrm{V}}(\vartheta;0,\omega_0)\sin(\vartheta)\ d\vartheta$ of the value $\overline{G}_{3\mathrm{V}}$ obtained above, where $\Phi_{4\mathrm{V}}(\vartheta;h_0,\omega_0)=\left|p(R\cos(\vartheta),R\sin(\vartheta);h_0,\omega_0)\right|^2$ is the square of the modulus of the sound pressure field of the pattern $\hat{\mathrm{S}}_{4\mathrm{V}}$ at the observation point $\{x=R\cos(\vartheta),\ z=R\sin(\vartheta)\}$ in the far zone (i.e., at $R>>L_0^2k_0$). Summing up the pressure of all monopoles at the observation point, we obtain

$$\overline{G}_{4\mathrm{V}}(h_0/k_0)=\frac{\int_0^{\pi}\sin(\vartheta)B^2(\mathrm{N},\ell,k_0,h_0,\vartheta)d\vartheta}{\int_0^{\pi}\sin(\vartheta)B^2(\mathrm{N},\ell,k_0,0,\vartheta)d\vartheta},\ \text{where}\ B(\mathrm{N},\ell,k_0,h_0,\vartheta)=\frac{\sin[(2\mathrm{N}+1)(k_0\cos(\vartheta)-h_0)\ell/2]}{\sin[(k_0\cos(\vartheta)-h_0)\ell/2]}.$$

As can be seen from fig. 5h, parameter $\overline{G}_{4\mathrm{V}}(h_0/k_0)$ of the pattern $\hat{\mathrm{S}}_{4\mathrm{V}}$ has no resonance at all (unlike $\overline{G}_3(h_0/k_0)$), although we set the amplitude of the spheres' oscillation velocity. In addition, $\overline{G}_{4\mathrm{V}}(h_0/k_0)$ approaches to a rectangular function at $k_0L_0\to\infty$, i.e. $\overline{G}_{4\mathrm{V}}(h_0/k_0)\underset{k_0L_0\to\infty}{\longrightarrow}[1-\mathbf{I}(h_0/k_0)]$. The reason for the qualitative difference of the value $\overline{G}_{4\mathrm{V}}(h_0/k_0)$ from $\overline{G}^{\mathrm{r}}_{3\mathrm{V}}(h_0/k_0)$ is, probably, that the mutual impedance of the pulsating rings spaced along the axis "x", putted on a rigid cylinder, is much greater than the mutual impedance of the pulsating spheres of the pattern $\hat{\mathrm{S}}_{4\mathrm{V}}$ separated by the medium at $ka<<1$ and $\ell>>a$ (if the spheres are small, then setting pressure on them or speed does not lead to a qualitative difference as between $\hat{\mathrm{S}}_{0\mathrm{V}}$ and $\hat{\mathrm{S}}_{0\mathrm{P}}$). On the other hand, it is obvious that a pattern $\hat{\mathrm{S}}_{5\mathrm{V}}$ in the form of a similar line of equidistant, but *two-dimensional* monopoles (i.e., pulsating cylinders parallel to the axis "y") must have the corresponding characteristic $\overline{G}_{5\mathrm{V}}(h_0/k_0)$, tending to $\overline{G}^{\mathrm{z}}_{0\mathrm{V}}(h_0/k_0)$ at $\mathrm{N}\to\infty$, i.e. $\overline{G}_{5\mathrm{V}}\underset{k_0L_0\to\infty}{\longrightarrow}\overline{G}^{\mathrm{z}}_{0\mathrm{V}}$, and the such pattern $\hat{\mathrm{S}}_{5\mathrm{V}}$ is a discrete version of the pattern $\hat{\mathrm{S}}_{0\mathrm{V}}$. In this case, the dimension (2D, 3D) of the boundary value problem plays a fundamental role. For example, if ℓ_0 is the distance between the centers of spheres and cylinders with radius R_0 ($k_0R_0<<1$, $\ell_0>>R_0$), then, at $k_0\ell_0>>1$, we obtain the ratio $\left|\hat{Z}_{2\mathrm{D}}\right|/\left|\hat{Z}_{3\mathrm{D}}\right|\approx\sqrt{\pi/2}\ \sqrt{\overline{\phi}/\overline{\overline{\phi}}}>>1$ of the modulus of mutual impedances of two parallel pulsing infinite cylinders $\left|\hat{Z}_{2\mathrm{D}}\right|$ and two pulsing spheres $\left|\hat{Z}_{3\mathrm{D}}\right|$, where $\overline{\phi}=\ell_0/R_0>>1$, $\overline{\overline{\phi}}=R_0k_0<<1$.

7. Conclusions

The dependence of the surface density of the wave power emitted by the pattern boundaries on the spatial frequency h_0 (in the mode of excitation of a phased antenna array for patterns $\hat{\mathrm{S}}_{0\mathrm{V}},\hat{\mathrm{S}}_{0\mathrm{Vg}},\hat{\mathrm{S}}_{0\mathrm{E}}$) and on the towing velocity U_0 (in the

mode of towing a static structure for patterns $\hat{S}_{0\tilde{V}}$, $\hat{S}_{0\tilde{V}g}$, $\hat{S}_{0\tilde{E}}$) has a pronounced resonant character and becomes infinite in points of resonance $h_0 = k_0$ and $U_0 = c_0$, where c_0 —the phase velocity of waves of the corresponding nature: sound waves (Section 1), waves on water (Section 2), electromagnetic waves (Section 3).

With appropriate excitation of the patterns $\hat{S}_{0V}$ (Section 4.1.1), $\hat{S}_{0Vg}$ (Section 4.1.2), $\hat{S}_{0E}$ (Section 4.1.3) (phased antenna array) or $\hat{S}_{0\tilde{V}}$, $\hat{S}_{0\tilde{V}g}$, $\hat{S}_{0\tilde{E}}$ (static structure towing, Section 4.2) at $|h_0| < k_0$ and $|U_0| > c_0$, a surface density of the tangential reaction force of the radiation field that is constant in time and along the boundary arises (opposite direction to phasor vector or towing velocity): respectively, the wave thrust force and the wave resistance force, proportional to the radiated power , i.e. with the same resonances $h_0 = k_0$ or $U_0 = c_0$.

In flat (2D) patterns $\hat{S}_{0V}$, $\hat{S}_{0Vg}$, $\hat{S}_{0E}$, $\hat{S}_{0\tilde{V}}$, $\hat{S}_{0\tilde{V}g}$, $\hat{S}_{0\tilde{E}}$ the tangential force of the radiation reaction is proportional only to the normal component of the Poynting vector, despite the fact that the tangential component of the Poynting vector in $\left[1-(h_0/k_0)^2\right]^{-1/2} >> 1$ times (patterns $\hat{S}_{0V}$, $\hat{S}_{0Vg}$, $\hat{S}_{0E}$) and in $\left[1-(c_0/U_0)^2\right]^{-1/2} >> 1$ times (patterns $\hat{S}_{0\tilde{V}}$, $\hat{S}_{0\tilde{V}g}$, $\hat{S}_{0\tilde{E}}$) exceeds normal component at $h_0 \to k_0$ and $U_0 \to c_0$.

The resonant radiation of grazing waves considered above by the boundary can be the cause of the following phenomena: (a) resonant radiation of air infrasound and the creation of wind by surface waves on sea surface; (b) tangential wave thrust of a phased antenna array (acoustic pump, thrust force of a plane current emitting a grazing wave, and vibration vehicle [17]); (c) deceleration of the flow by radiation of surface waves by a wavy coast at a "resonant" speed $U_0 \to \sqrt{g_0 / H_0}$, deceleration by radiation of a towed body in air at (wave crisis or sound barrier [20]); (d) deceleration by radiation of a towed sinusoidal static structure of the charge density (Vavilov-Cherenkov radiation [22]).

The finite size ($L_0 < \infty$, $R_0 = \infty$, $\hat{S}_{1V}$, Section 6.1) and the finite curvature (convexity, $R_0 < \infty$, $L_0 = \infty$, $\hat{S}_{2V}$ (Section 6.2.1), $\hat{S}_{3V}$ (Section 6.2.2)) of the pattern lead to a finite value of the resonant radiation peak, since reduce the interaction between the elements of the surface of the pattern through the field. In the traditional version of a traveling wave acoustic antenna in the form of equidistant pulsating spheres separated by a waveguide medium (pattern $\hat{S}_{4V}$), resonance is completely absent together with the absence of interaction between the elements via the field.

Acknowledgments

This work was supported by the Project FFUF-2021-0009 of the Institute of Applied Physics (RAS).

References

[1] John William Strutt Rayleigh. The Theory of Sound; Volume 2, Franklin Classics, 978-0341849094, 2018.

[2] Landau L.D., Lifshitz E.M. Course of theoretical physics (Fluid Mechanics), Vol. 6, Butterworth-Heinemann, 2nd edition., January 15, 1987, http://users.uoa.gr/~pjioannou/mechgrad/Chap_1_Landau_Lifschitz_FM.pdf.

[3] Eugen Skudrzyk. The Foundations of Acoustics (Basic Mathematics and Basic Acoustics), Springer, 1971.

[4] James Lighthill. Waves in fluids, Cambridge University Press, London, New York, Melbourne, 1978.

[5] Sretensky L. N. Theory of wave motions of a liquid [M]. Nauka, 1977 (in Russian).

[6] John D. Jackson. Classical electrodynamics. New York: Wiley, 1999.

[7] Carlton H. Walter. Travelling wave antennas. Peninsula Pub, June 1, 1990, ISBN: 9780932146519.

[8] Lim Chee-Seng. A Class of Problems of Pulsatory Radiation from a Travelling Source Distribution. SIAM Journal on Applied Mathematics, 1988. V. 48, No. 2. P. 326-352. https://doi.org/10.1137/0148017.

[9] Isakovich M.A. General acoustics. Moscow: Nauka 1973 (in Russian).

[10] Arabadzhi V. V. Solutions to problems of controlling long waves with the help of micro-structure tools. Sharjah: Bentham Science Publishers, 2011. P. 187. doi: 9781608053698.

[11] Arabadzhi V. V. Resonant radiation of boundary with a travelling distribution of the field. Journal of Engineering Research and Sciences. 2022. V. 1, No. 4. P. 1-8. doi:10.55708/js0104001.

[12] Markov G.N., Chaplin A.F. Excitation of electromagnetic waves. Moscow: Energy, 1967 (in Russian).

[13] Mc-Intire M. E. On the 'wave momentum' myth//J. Fluid Mech. 25-th Anniversary issue, 1981, vol. 106, pp. 331-347.

[14] Lebedew P., Annalen der Physik. 1901. fasc. 4, Bd 6, S. 433-458. doi: https://dx.doi.org/10.1002/andp.19013111102.

[15] Hasegawa T, Kido T, Iizuka T, Matsuoka C. "A general theory of Rayleigh and Langevin radiation pressures". The Journal of the Acoustical Society of Japan (E), (2000), 21 (3): 145-152. doi:10.1250/ast.21.145. ISSN 0388-2861.

[16] Beyer R.T. "Radiation pressure—The history of a mislabeled tensor," J. Acoust. Soc. Am. 63, 1025-1030 (1978). https://www.ece.uvic.ca/~bctill/papers/numacoust/Beyer_1978.pdf.

[17] Blekhman I. I. Vibration mechanics. Moscow: Fizmatlit, 1994 (in Russian).

[18] Rzhevkin S. N. Lectures on the theory of sound. M.: Ed. Moscow State University, 1960 (in Russian).

[19] B. M. Budak, A. A. Samarskii, A. N. Tikhonov. A Collection of Problems on Mathematical Physics Elsevier, 2013.

[20] Anderson John D. Jr. Fundamentals of Aerodynamics. N-Y.: McGraw-Hill, 2017. 1130 p.

[21] J.N. Newman, Marine Hydrodynamics the MIT Press, Cambridge Massachusetts, 1935, https://archive.org/details/marinehydro-dynam0000newm.

[22] Bolotovskii B.M. Vavilov-Cherenkov radiation: its discovery and application. Physics Uspekhi, vol. 52, issue 11, PP. 1099-1110, 2009, doi: 10.3367/UFNe.0179.200911c.1161.